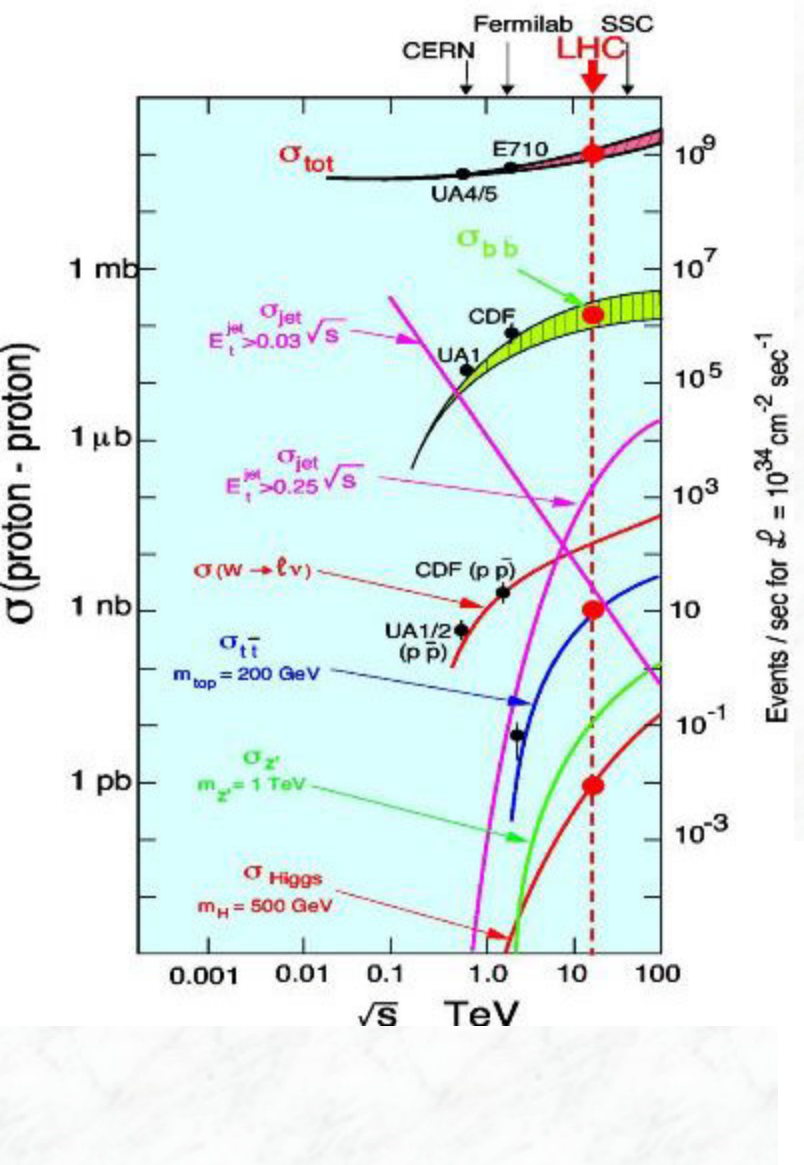


3. Towards Physics: Reconstruction and Kinematics

- 3.1 Event selection, Trigger
- 3.2 First results on the performance of the LHC detectors

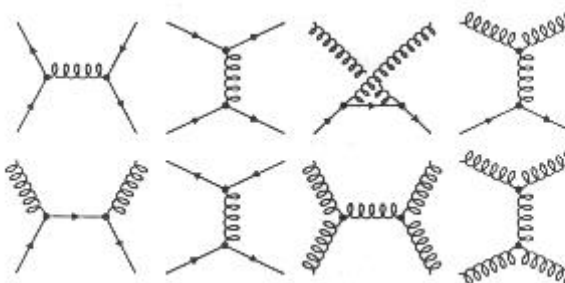
- 3.3 Relativistic Kinematics (repetition from Particle Physics II)
- 3.4 Important variables for pp collisions

Erwartete Produktionsraten am LHC



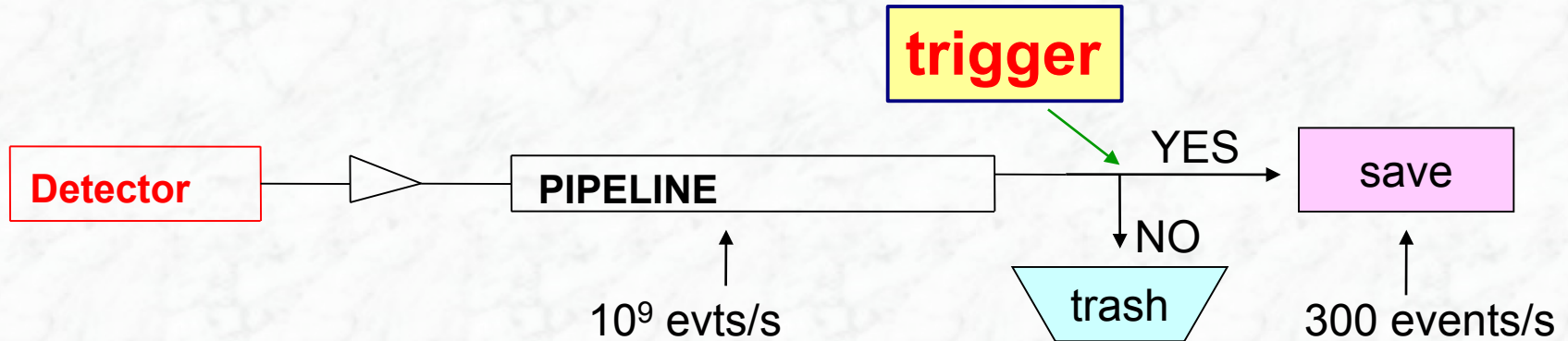
| | |
|--|---------------------------|
| • Inelastische Proton-Proton Reaktionen: | 1 Milliarde / sec |
| • Quark - Quark/Gluon Streuungen mit großen transversalen Impulsen | ~ 100 Millionen/ sec |
| • b-Quark Paare | 5 Millionen / sec |
| • Top-Quark Paare | 8 / sec |
| • $W \rightarrow e \nu$ | 150 / sec |
| • $Z \rightarrow e e$ | 15 / sec |
| • Higgs (150 GeV) | 0.2 / sec |
| • Gluino, Squarks (1 TeV) | 0.03 / sec |

Dominante harte Streuprozesse: Quark - Quark
Quark - Gluon
Gluon - Gluon



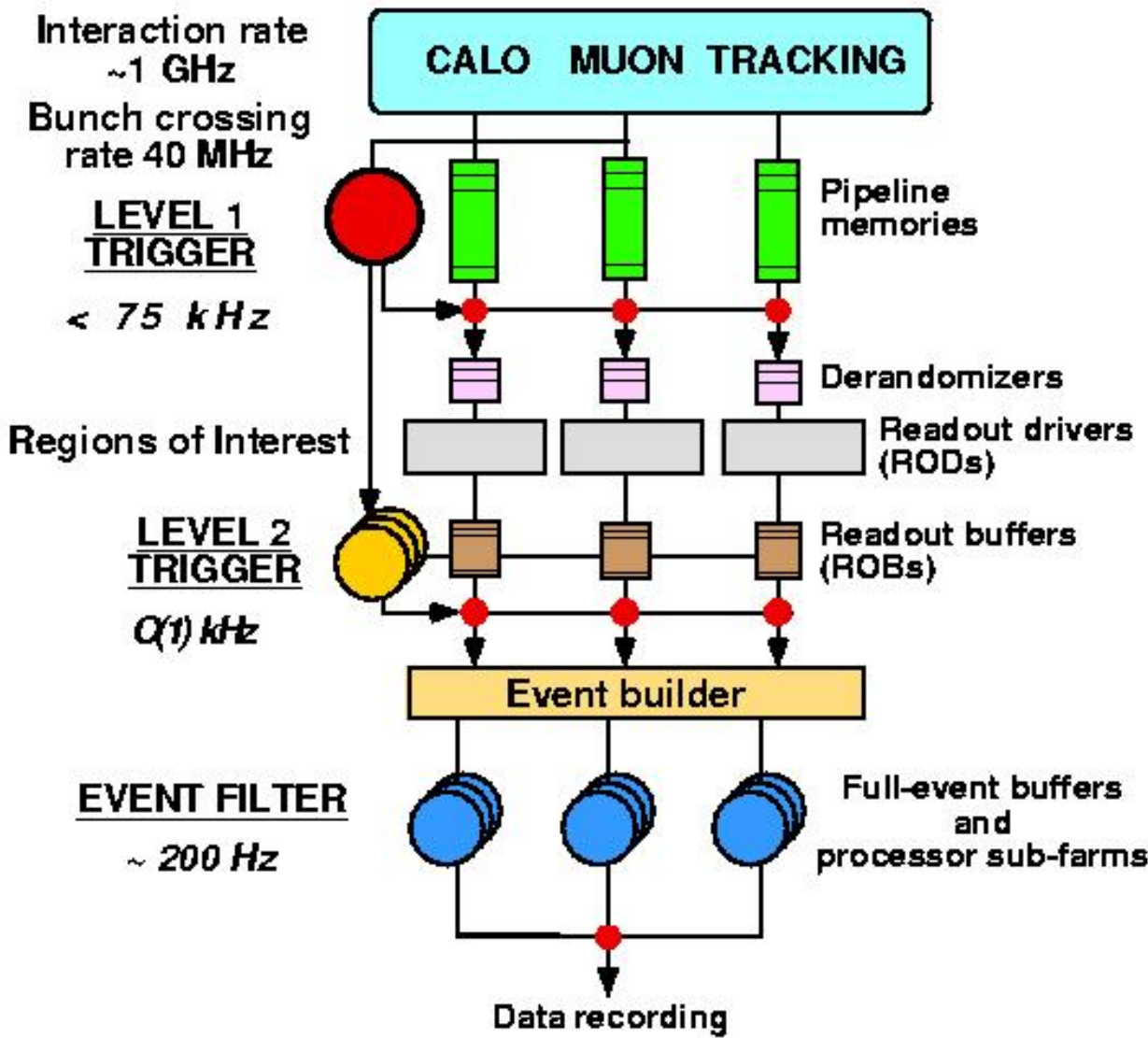
How to Select Interesting Events?

- Bunch crossing rate: 40 MHz, ~25 interactions per BX (10^9 events/s)
 - can only record ~1000 event/s (~1 MB each), still 1 GB/s data rate
- Need highly efficient and highly selective TRIGGER
 - raw event data (70 TB/s) are stored in pipeline until trigger decision



- ATLAS trigger has 3 levels (CMS similar with 2 levels)
 - Level-1: hardware, ~2.5 μ s decision time,
40 MHz → 100 kHz
 - High-level trigger: software (O(20k cores)), ~200 ms decision time,
100 kHz → 1 kHz

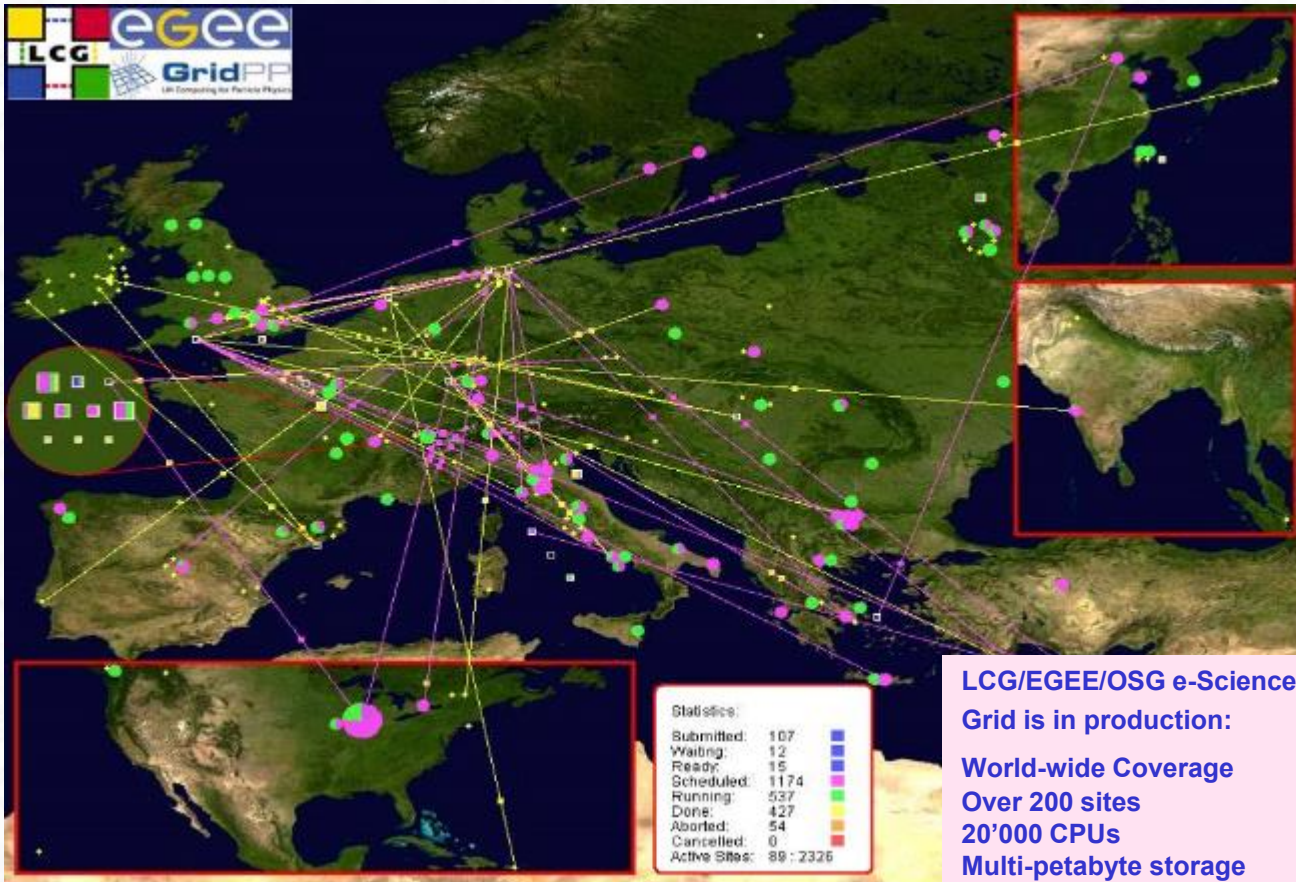
ATLAS Trigger System



Main trigger objects:
at Level 1:

- e/ γ clusters (calo)
- Muons (muon)
- Jets (high p_T , calo)
- Missing transverse energy (calo)

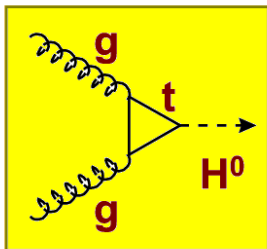
LHC data handling, GRID computing



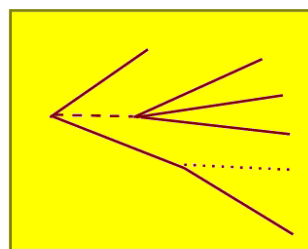
**Trigger system selects
~1000 “collisions” per sec.**

**LHC data volume per year:
10-15 Petabytes**
= $10-15 \cdot 10^{15}$ Byte

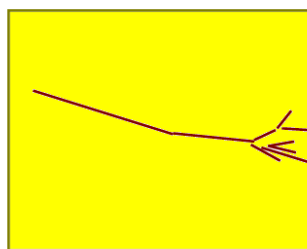
From Physics to Raw Data



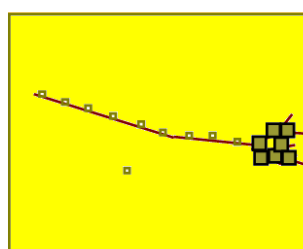
Basic physics



**Fragmentation,
Decay**



**Interaction with
detector material
Multiple scattering,
interactions**



**Detector
response
Noise, pile-up,
cross-talk,
inefficiency,
ambiguity,
resolution,
response
function,
alignment**

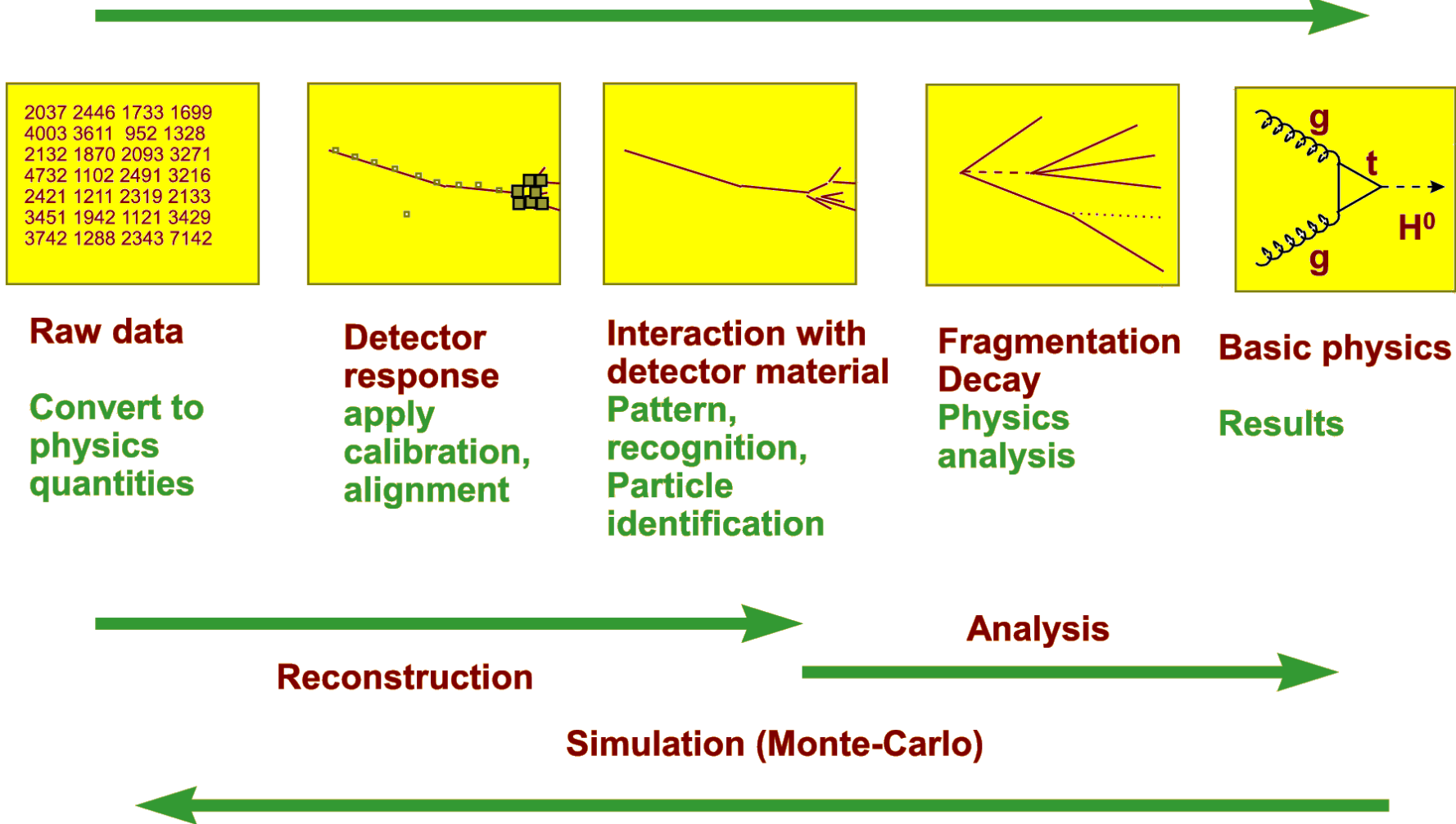
| |
|--|
| 2037 2446 1733 1699 4003 3611 952 1328 2132 1870 2093 3271 4732 1102 2491 3216 2421 1211 2319 2133 3451 1942 1121 3429 3742 1288 2343 7142 |
|--|

Raw data

**Read-out
addresses,
ADC, TDC
values,
Bit patterns**

- Actually recorded are raw data with ~1 GB/s for ATLAS and CMS
 - mainly electronics numbers
 - e.g. number of a detector element where the ADC (Analog-to-Digital converter) measured a signal with x counts...

From Raw Data To Physics



- We need to go from raw data back to physics
→ reconstruction + analysis of the event(s)

Towards Physics: some aspects of reconstruction of physics objects

- As discussed before, key signatures at Hadron Colliders are

Leptons: e (tracking + very good electromagnetic calorimetry)
μ (dedicated muon systems, combination of inner tracking and muon spectrometers)
τ hadronic decays: $\tau \rightarrow \pi^+ + n \pi^0 + \nu$ (1 prong)
 $\rightarrow \pi^+ \pi^- \pi^+ + n \pi^0 + \nu$ (3 prong)

Photons: γ (tracking + very good electromagnetic calorimetry)

Jets: electromagnetic and hadronic calorimeters
b-jets identification of b-jets (b-tagging) important for many physics studies

Missing transverse energy: inferred from the measurement of the total energy in the calorimeters; needs understanding of all components... response of the calorimeter to low energy particles

Requirements on e/γ Identification in ATLAS/CMS

● Electron identification

★ Isolated electrons: e/jet separation

- $R_{jet} \sim 10^5$ needed in the range $p_T > 20$ GeV
- $R_{jet} \sim 10^6$ for a pure electron inclusive sample ($\varepsilon_e \sim 60\text{-}70\%$)

★ Soft electron identification – e/π separation

- B physics studies (J/ψ)
- Soft electron b-tagging (WH, ttH with $H \rightarrow bb$)

● Photon identification

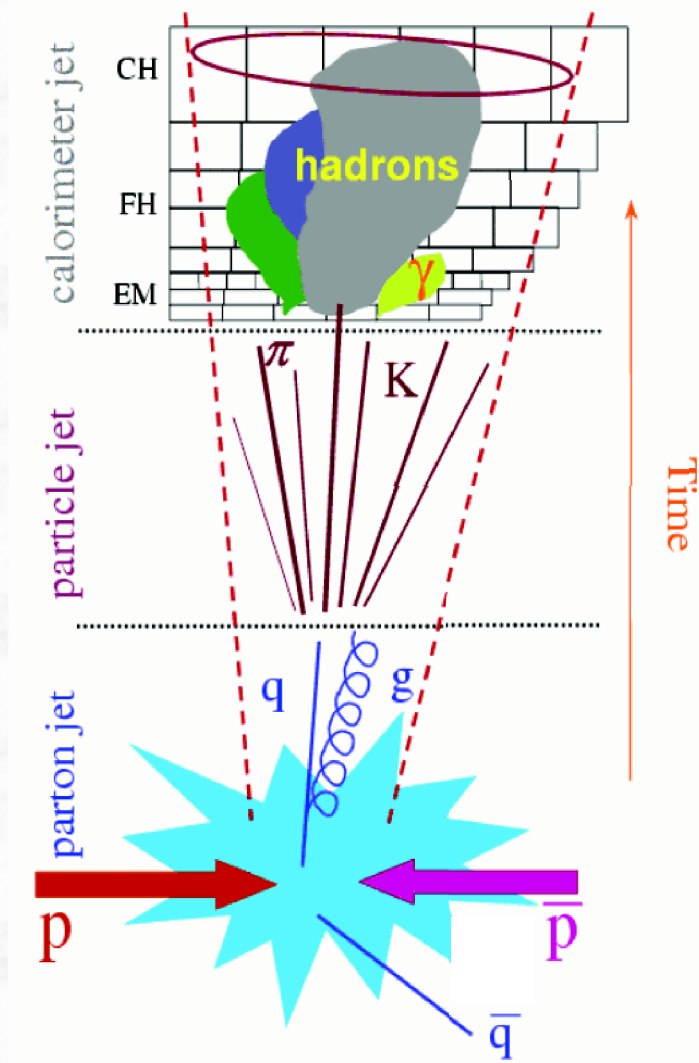
★ γ /jet and γ/π^0 separation

- Main reducible background to $H \rightarrow \gamma\gamma$ comes from jet-jet and is $\sim 2 \cdot 10^6$ larger than signal
- $R_{jet} \sim 5000$ in the range $E_T > 25$ GeV
- R (isolated high- $p_T \pi^0$) ~ 3

★ Identification of conversions

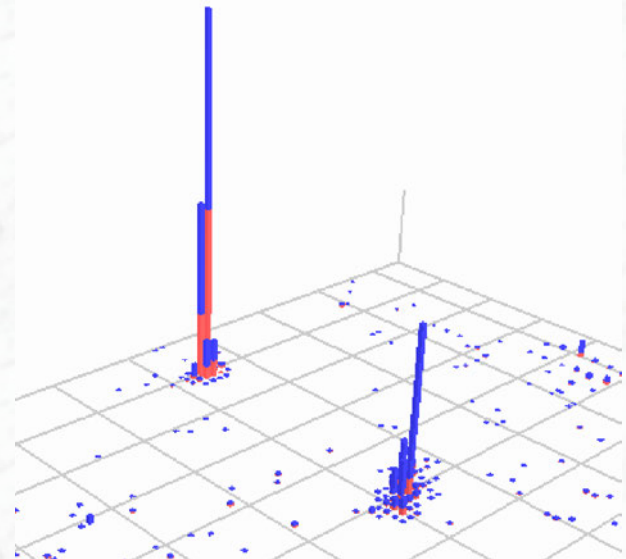
Jet reconstruction and energy measurement

- A jet is NOT a well defined object
(fragmentation, gluon radiation, detector response)
- The detector response is different for particles interacting electromagnetically (e, γ) and for hadrons
→ for comparisons with theory, one needs to correct back the calorimeter energies to the „particle level“ (particle jet)
Common ground between theory and experiment
- One needs an algorithm to define a jet and to measure its energy
conflicting requirements between experiment and theory (exp. simple, e.g. cone algorithm, vs. theoretically sound (no infrared divergencies))
- Energy corrections for losses of fragmentation products outside jet definition and underlying event or pileup energy inside

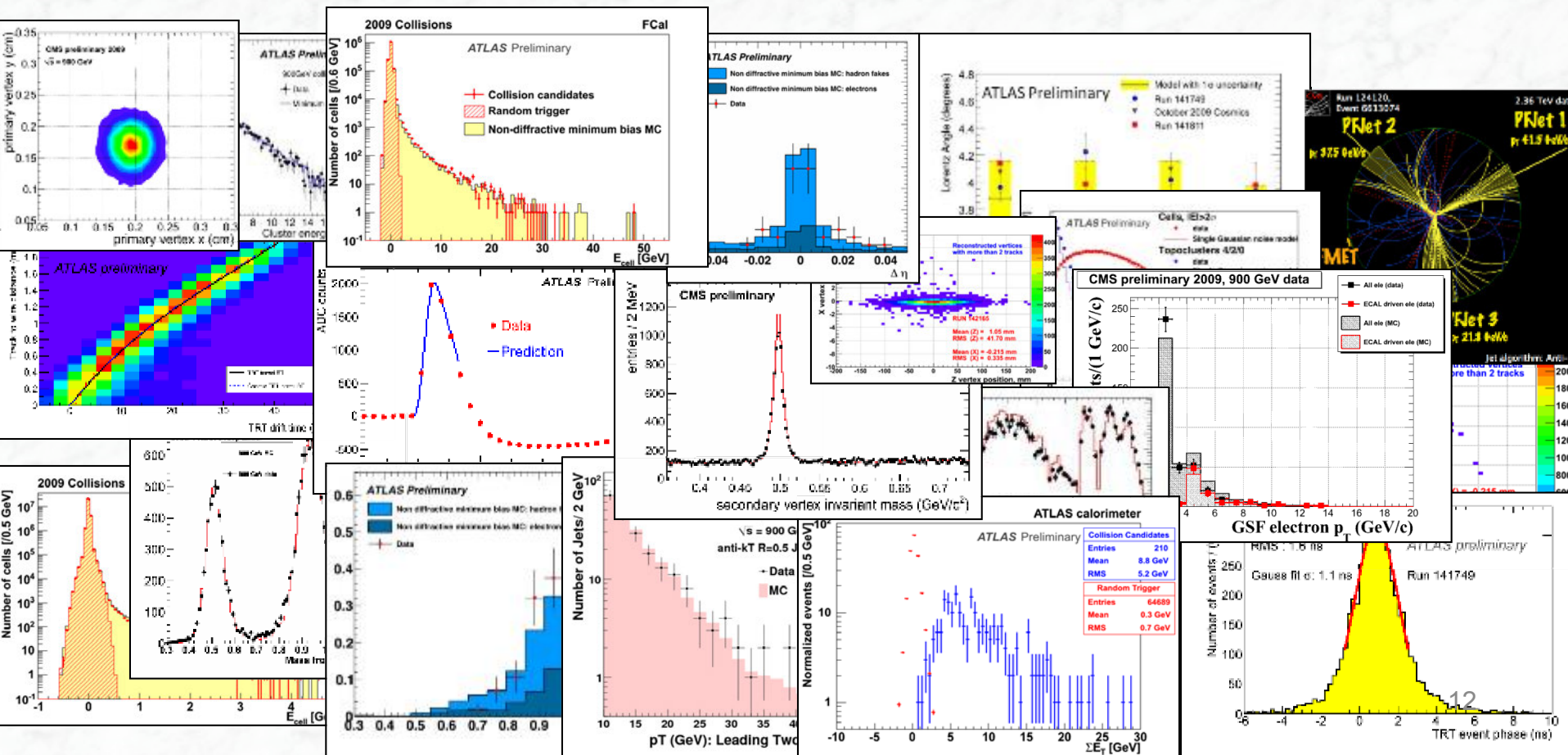


Main corrections:

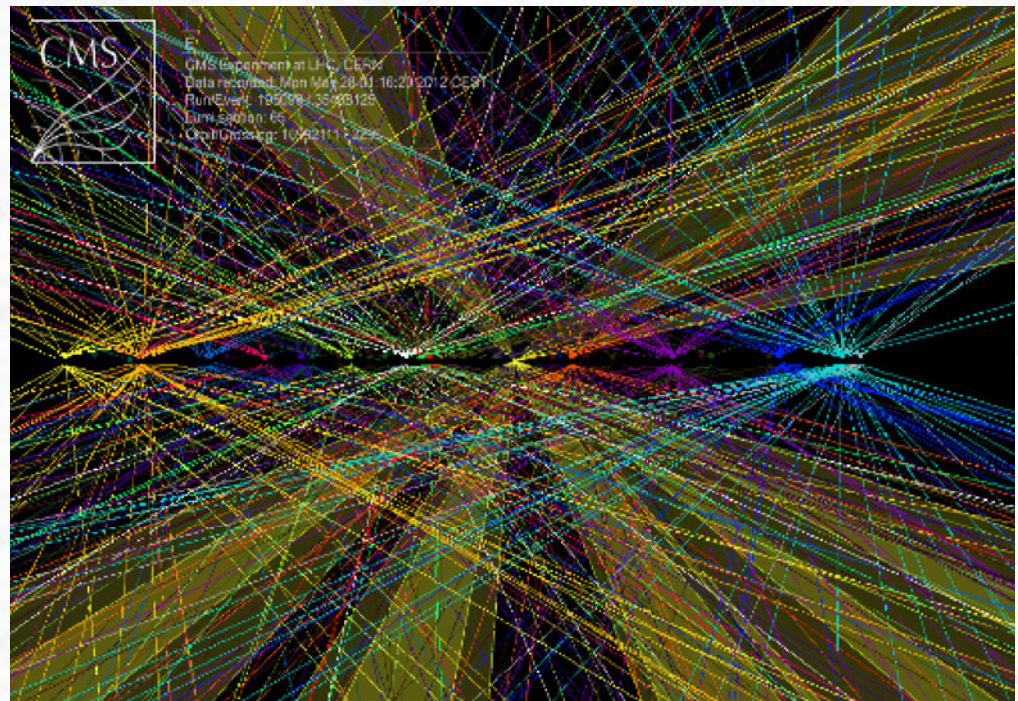
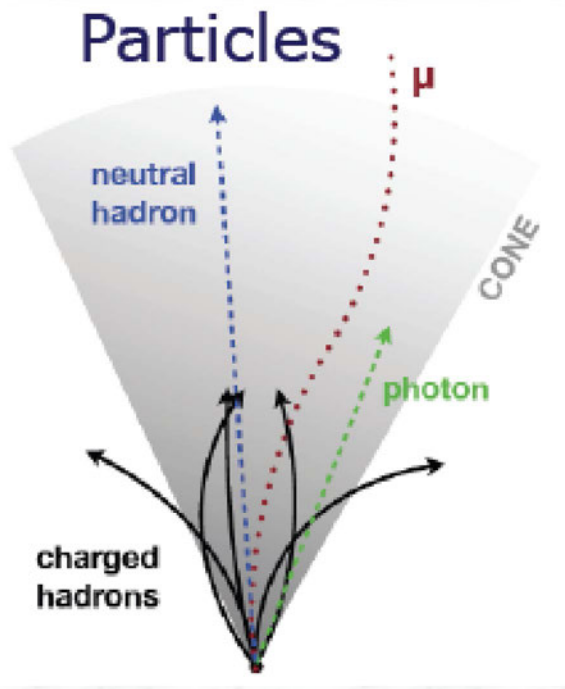
- In general, calorimeters show different response to electrons/photons and hadrons
- Subtraction of offset energy not originating from the hard scattering
(inside the same collision or pile-up contributions, use minimum bias data to extract this)
- Correction for jet energy out of cone
(corrected with jet data + Monte Carlo simulations)



3.2 First results on the performance of the LHC Detectors



3.2 Detector Performance

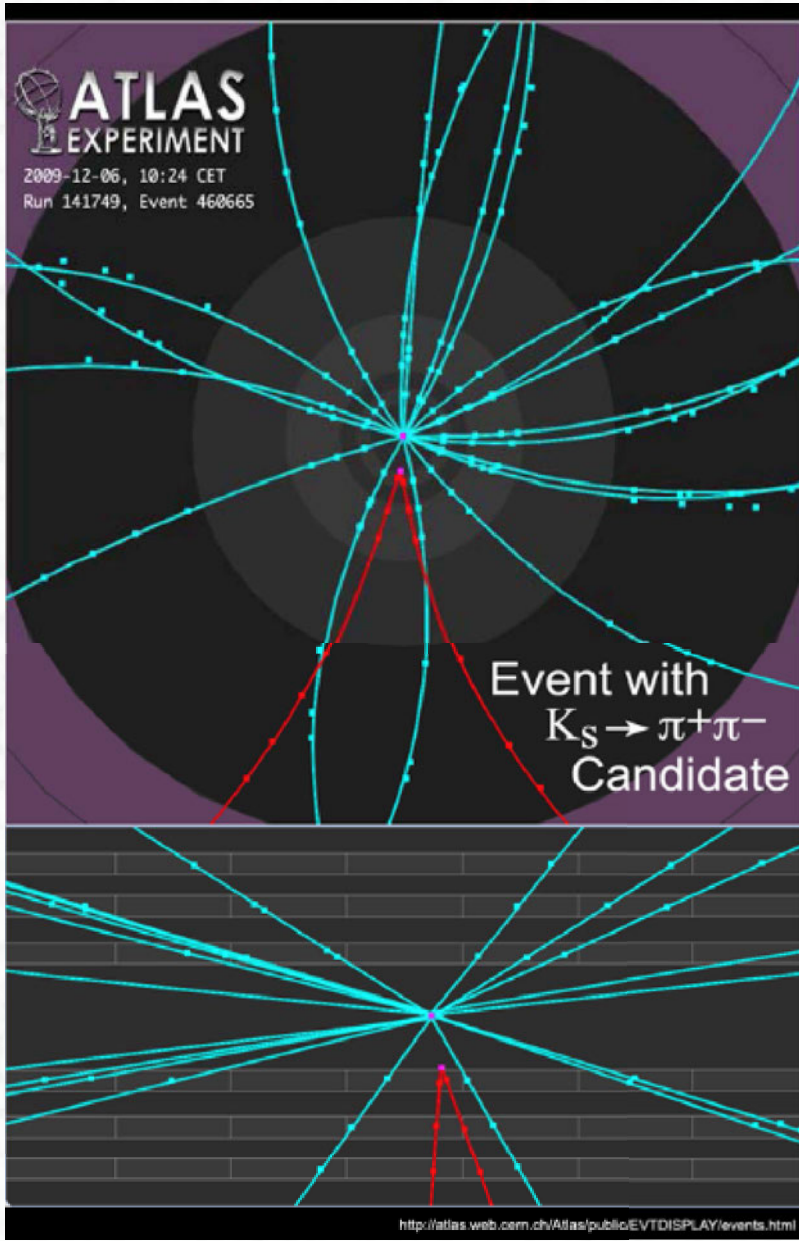


Detector Hardware Status in 2010



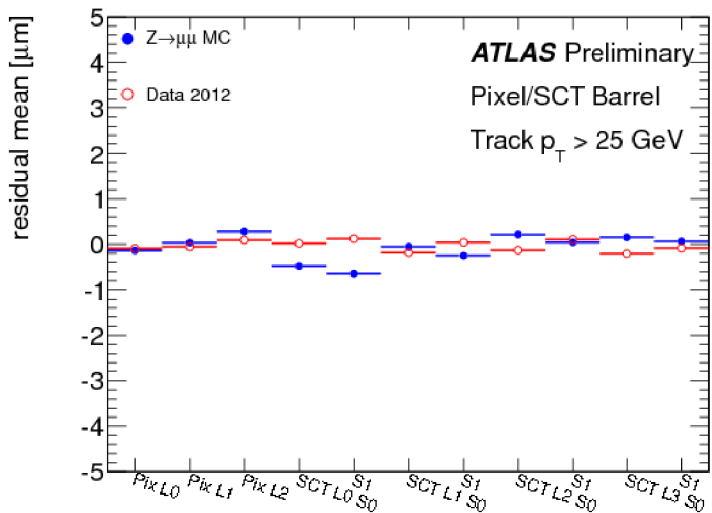
| Subdetector | Number of Channels | Operational Fraction |
|----------------------------------|--------------------|----------------------|
| Pixels | 80 M | 97.9% |
| SCT Silicon Strips | 6.3 M | 99.3% |
| TRT Transition Radiation Tracker | 350 k | 98.2% |
| LAr EM Calorimeter | 170 k | 98.8% |
| Tile calorimeter | 9800 | 99.2% |
| Hadronic endcap LAr calorimeter | 5600 | 99.9% |
| Forward LAr calorimeter | 3500 | 100% |
| MDT Muon Drift Tubes | 350 k | 99.7% |
| CSC Cathode Strip Chambers | 31 k | 98.4% |
| RPC Barrel Muon Trigger | 370 k | 98.5% |
| TGC Endcap Muon Trigger | 320 k | 99.4% |
| LVL1 Calo trigger | 7160 | 99.8% |

Very small number of non-working detector channels (out of several millions) in both experiments

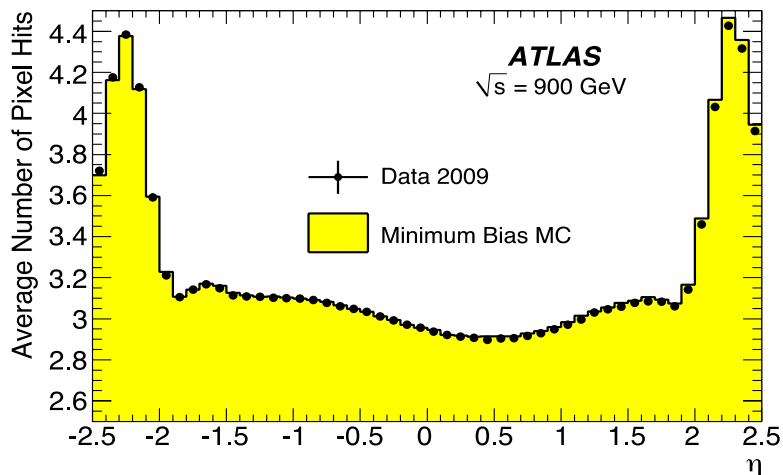


Tracking

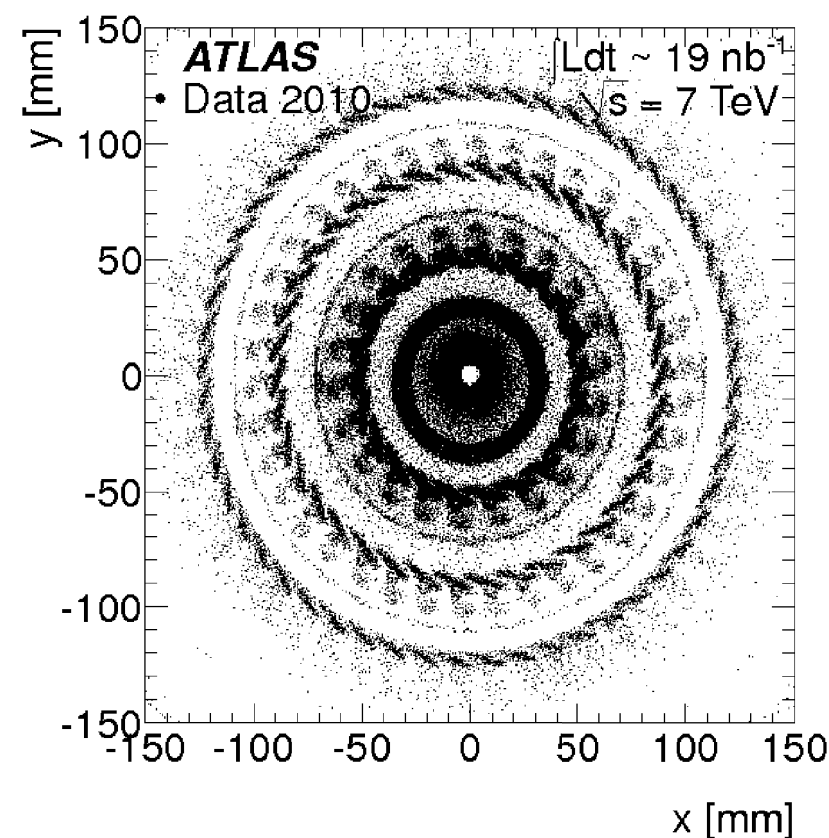
(i) Inner Detector performance: hits, tracks,...



Very good alignment of the silicon detector modules



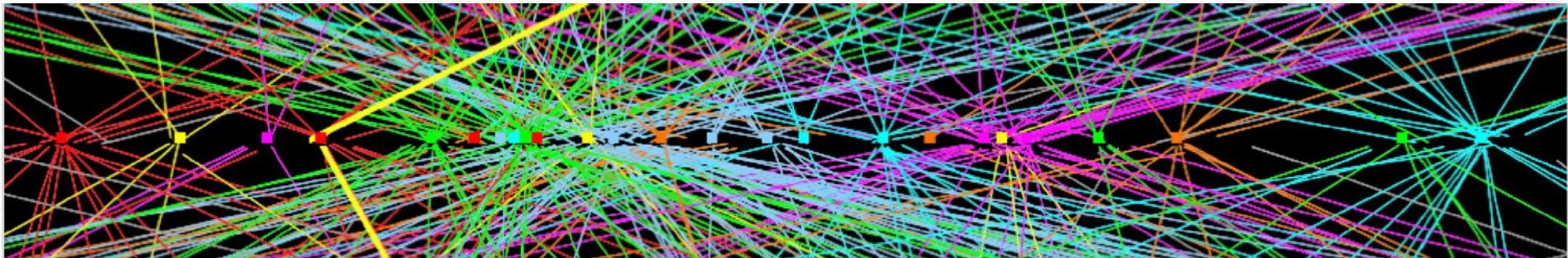
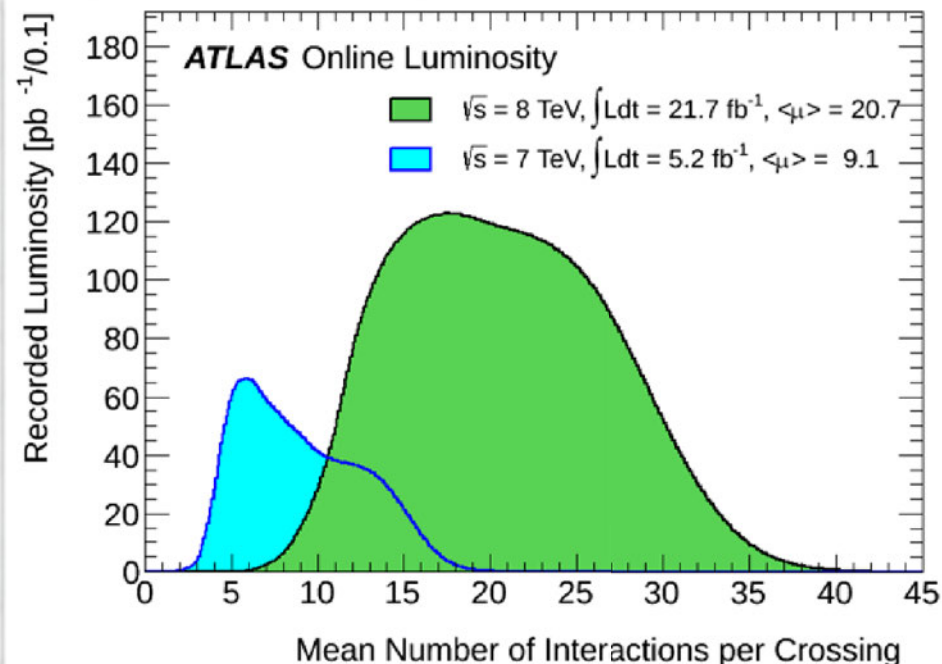
Very good agreement between data and Monte Carlo for the average number of hits on track



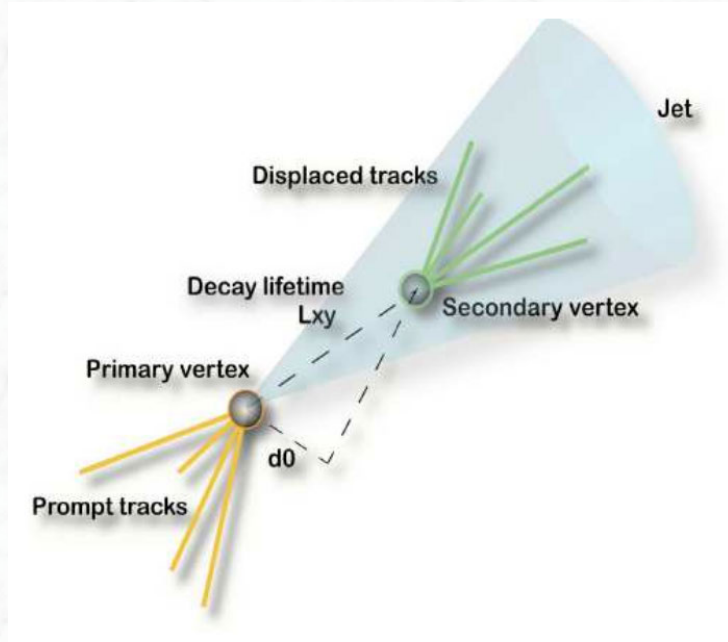
Secondary vertices for “x-ray” images of the detector material

Pile-up:

- **In-time pile-up:**
simultaneous pp interactions in
the same bunch crossing
- **Out-of-time pile-up:**
Time resolution of some sub-
detectors >25 ns, thus,
integrate measurement from
several bunch crossings

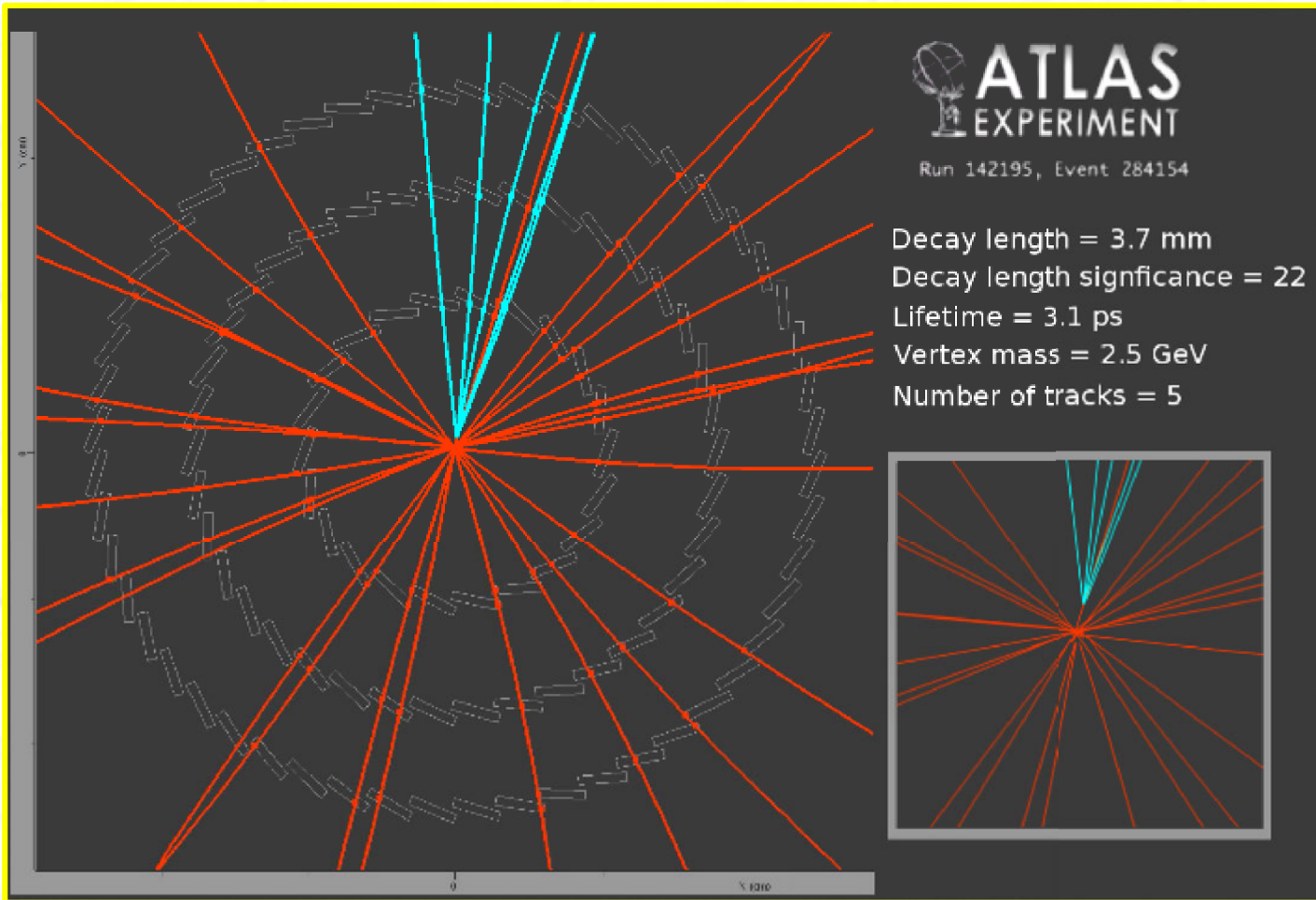


(ii) How well can b-quarks be tagged ?



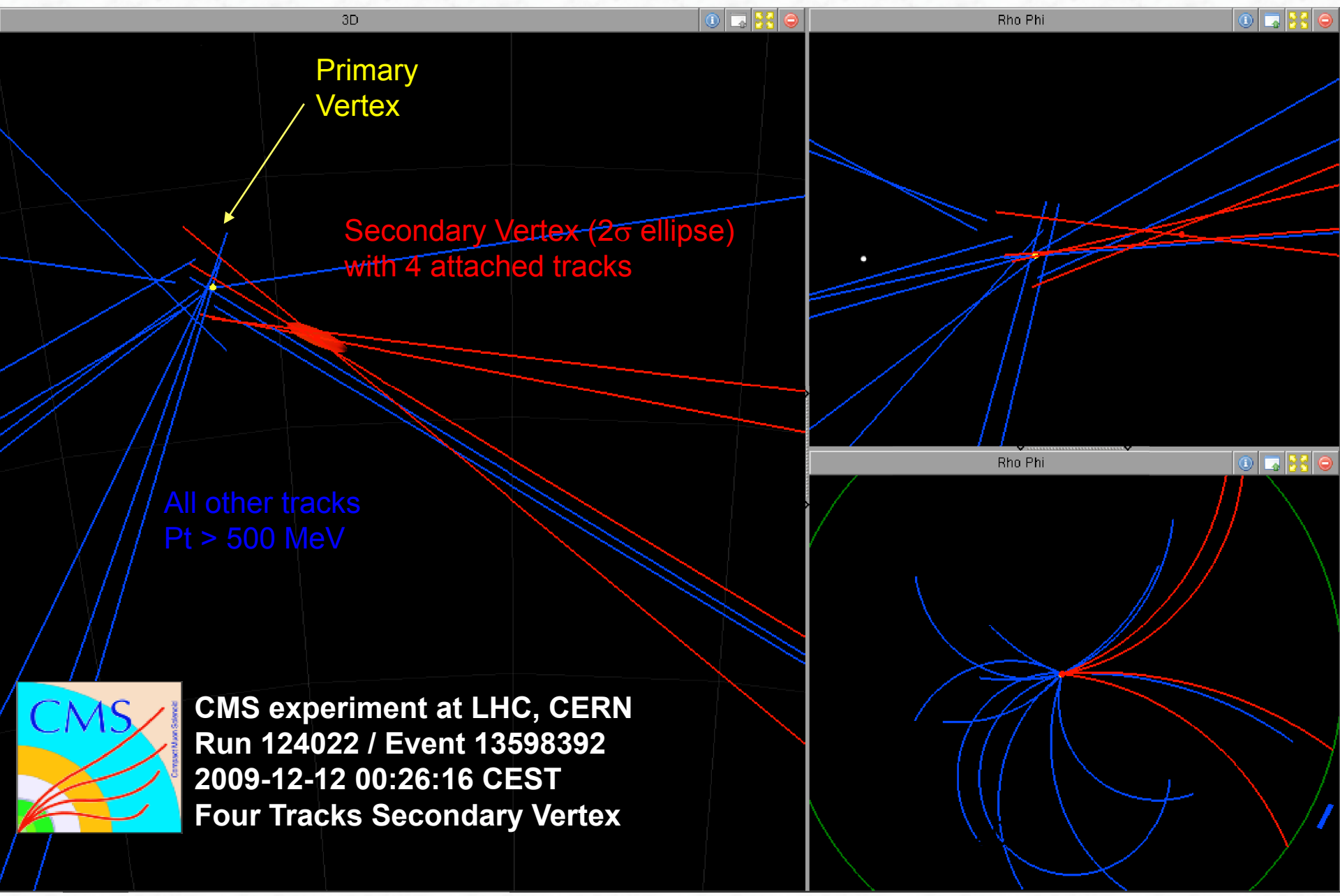
- b quarks fragment into B hadrons (mesons and baryons)
 - B mesons have a lifetime of ~ 1.5 ps
They fly in the detector about 2-3 mm before they decay
- reconstruction of a secondary vertex possible
(requires high granularity silicon pixel and strip detectors close to the interaction point)
- tracks from B meson decays have a large impact parameter w.r.t. the primary vertex

.... towards b-tagging

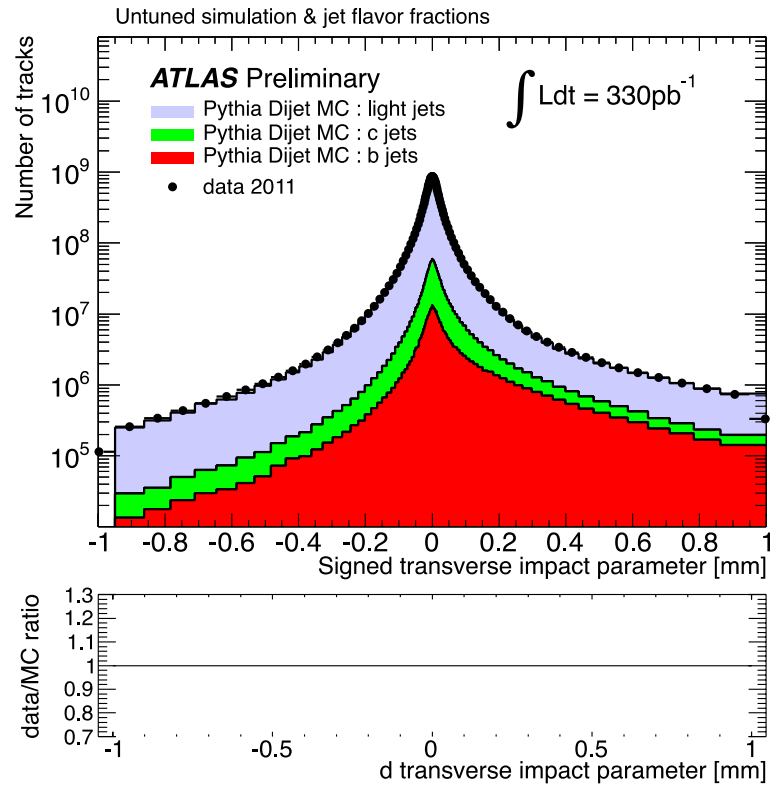


An example of a jet tagged with the secondary vertex tagger (SV0)
(Light jet probability: 10^{-4})

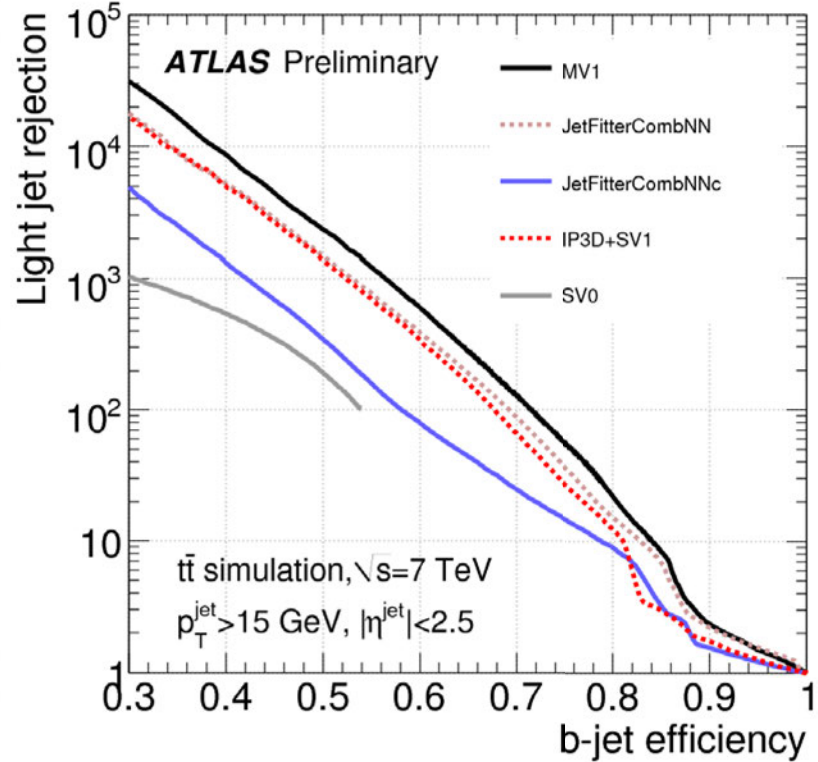
.... CMS b-tagged candidate event



ATLAS results on b-tagging performance:

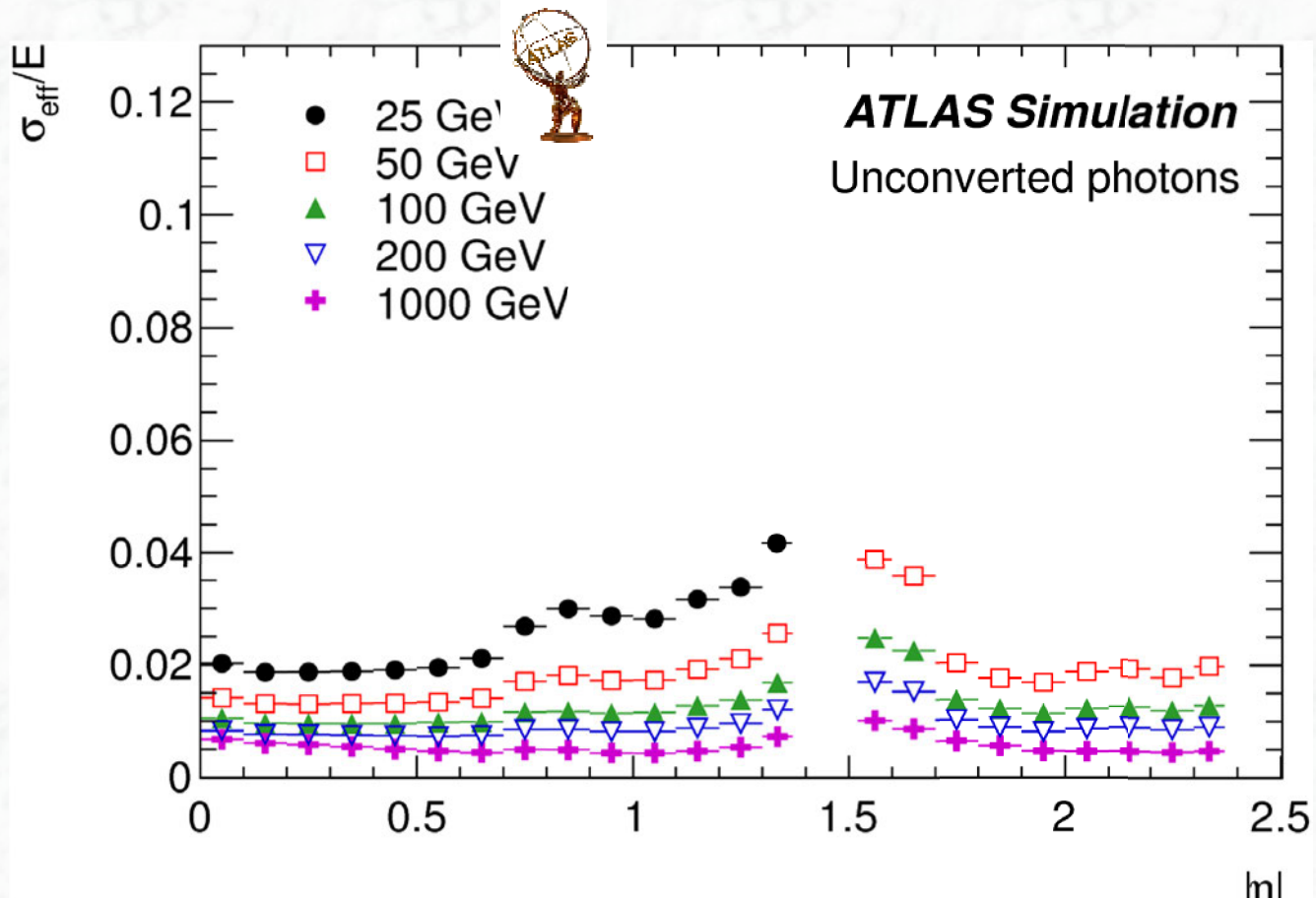


Distribution of the signed transverse impact parameter with respect to primary vertex for tracks of b-tagging quality associated to jets, for experimental data (solid black points) and for simulated data (filled histograms for the various flavors). The ratio data/simulation is shown at the bottom of the plot.



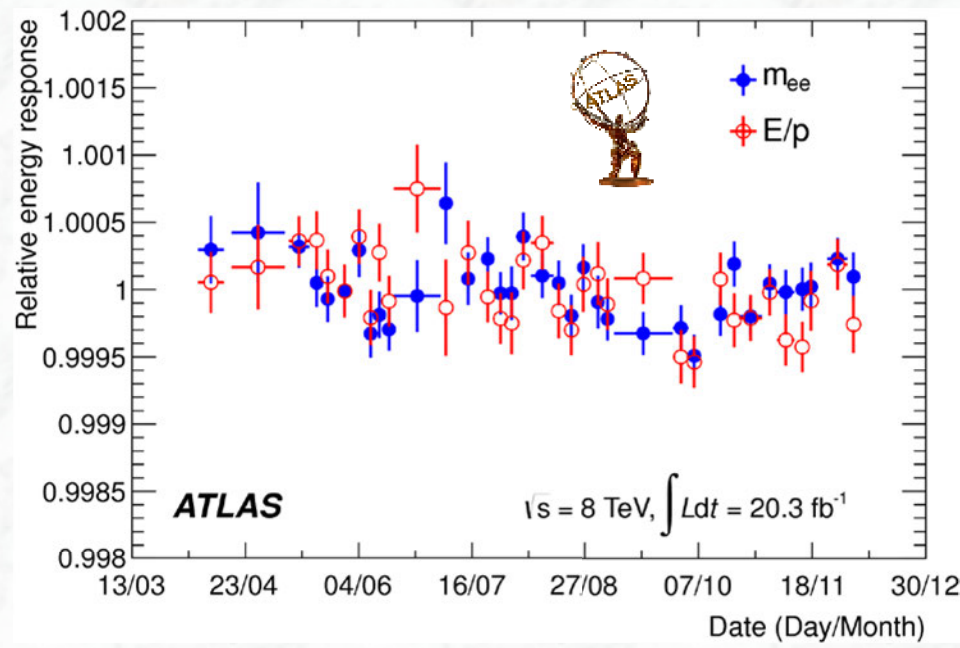
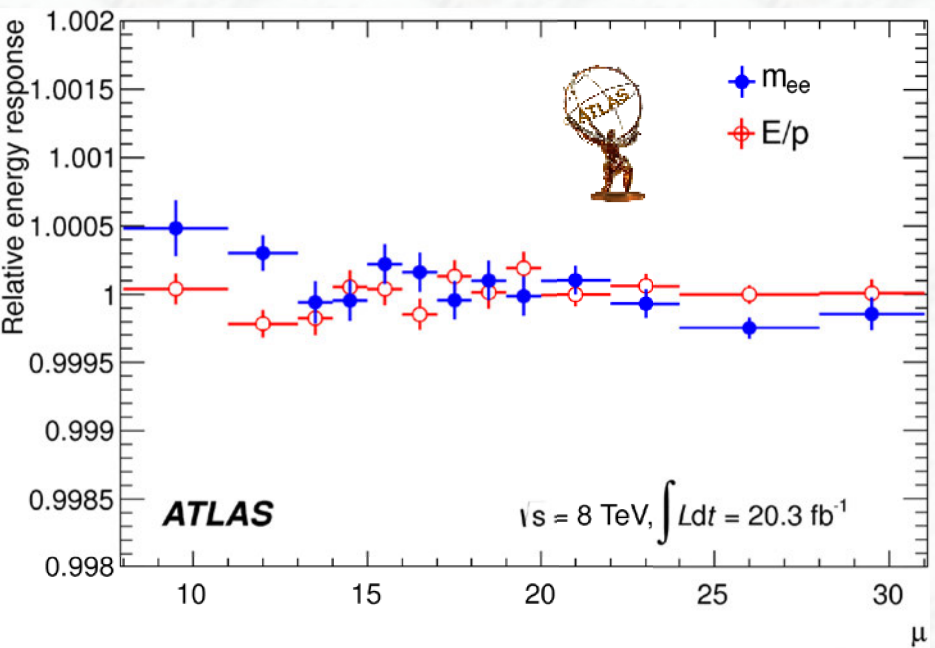
Light-jet rejection as a function of the b-jet tagging efficiency for the early tagging algorithms (IP3D+SV1 and SV0) and for the high performance algorithms, based on simulated top-antitop events.

(iii) Some performance figures on photons from 2012 data:



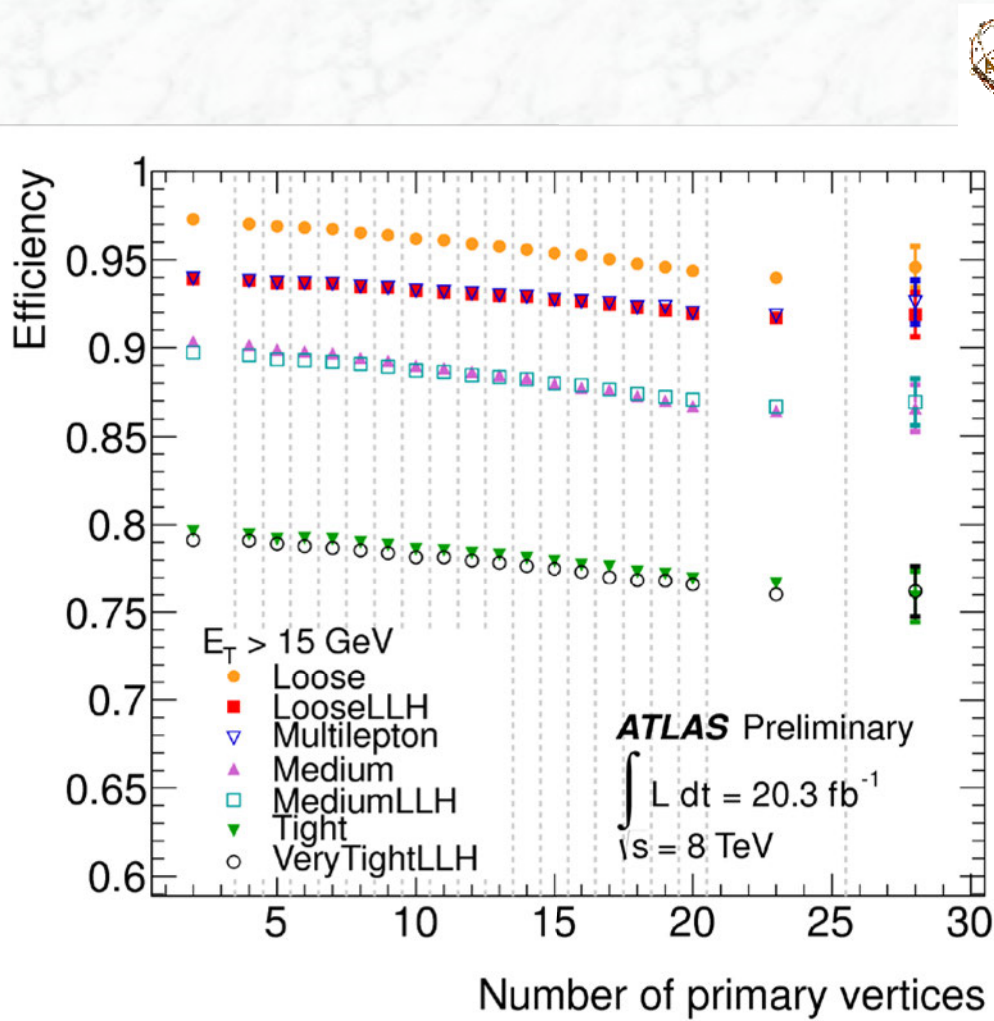
Energy resolution of unconverted photons in ATLAS
(compare to calorimetry lecture)

(iii) Some performance figures on electrons from 2012 data:

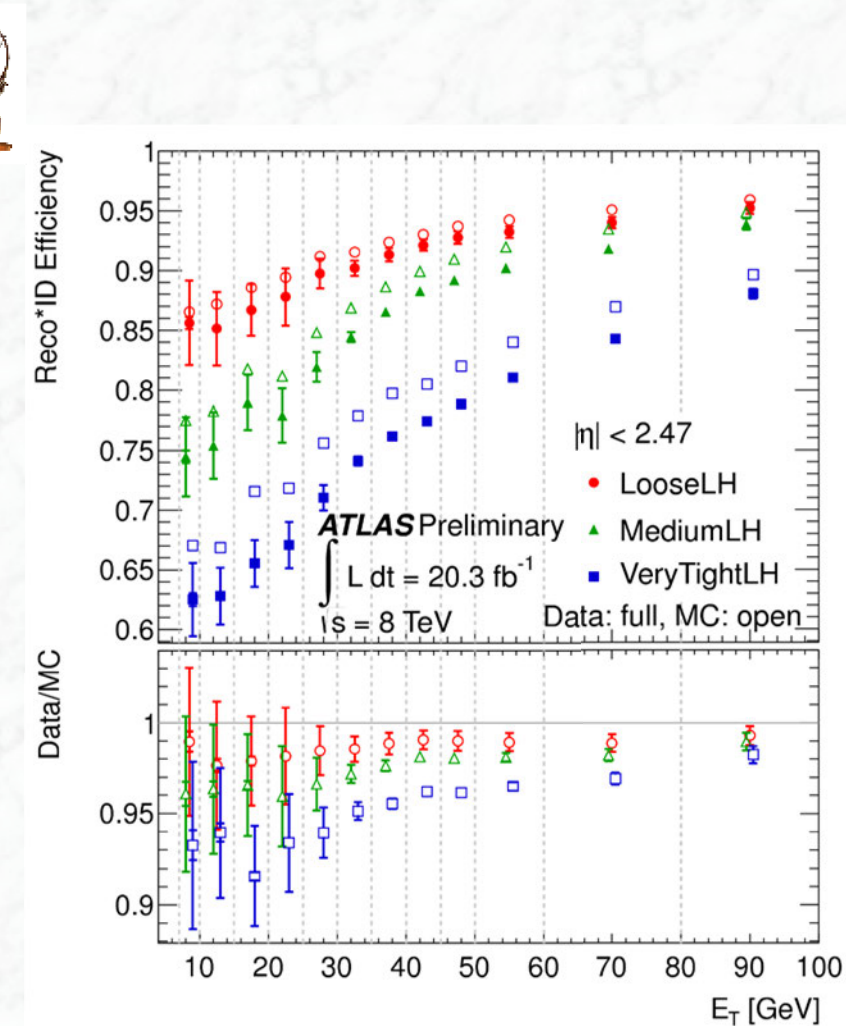


Electron energy response stability in ATLAS

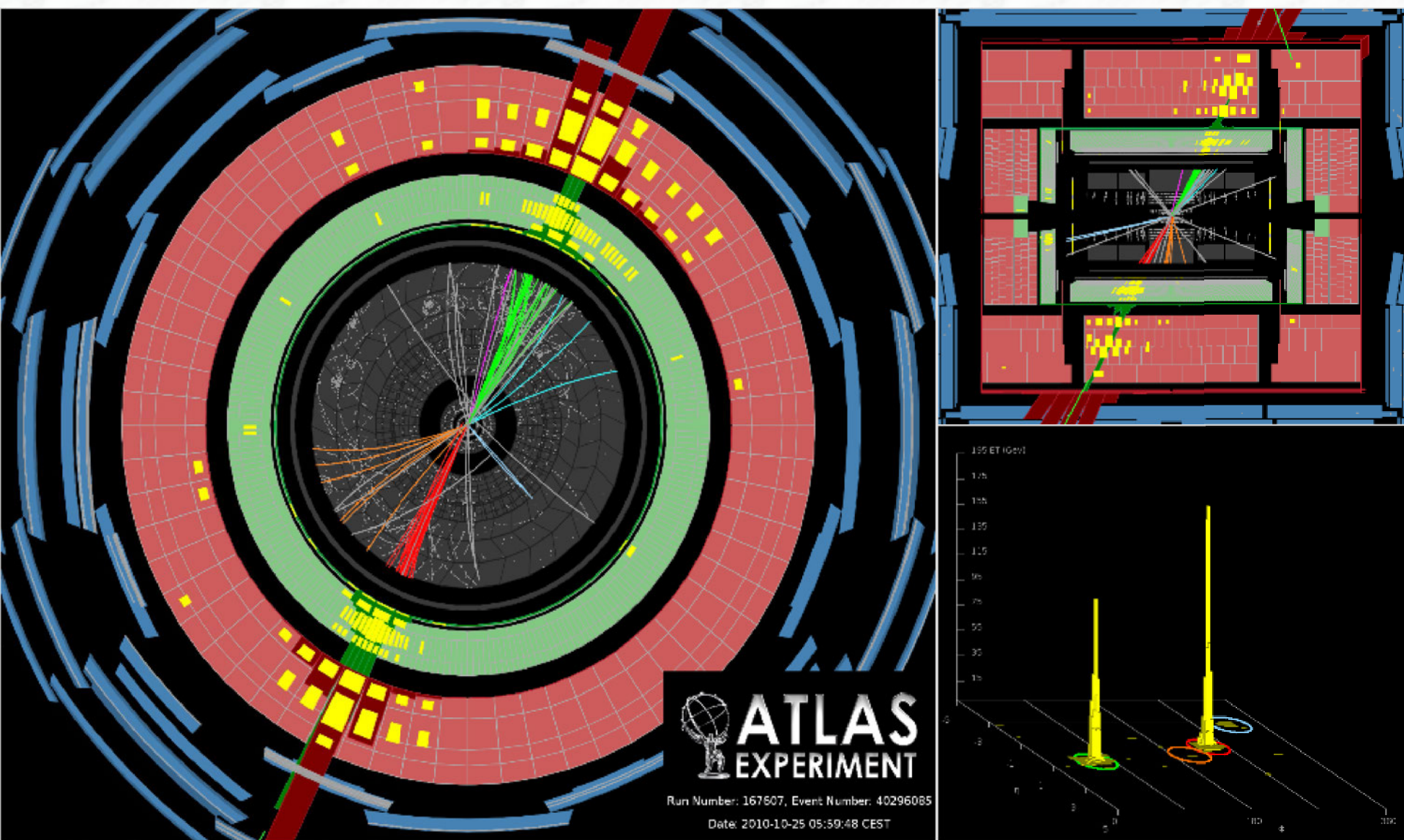
(iii) Some performance figures on electrons from 2012 data:



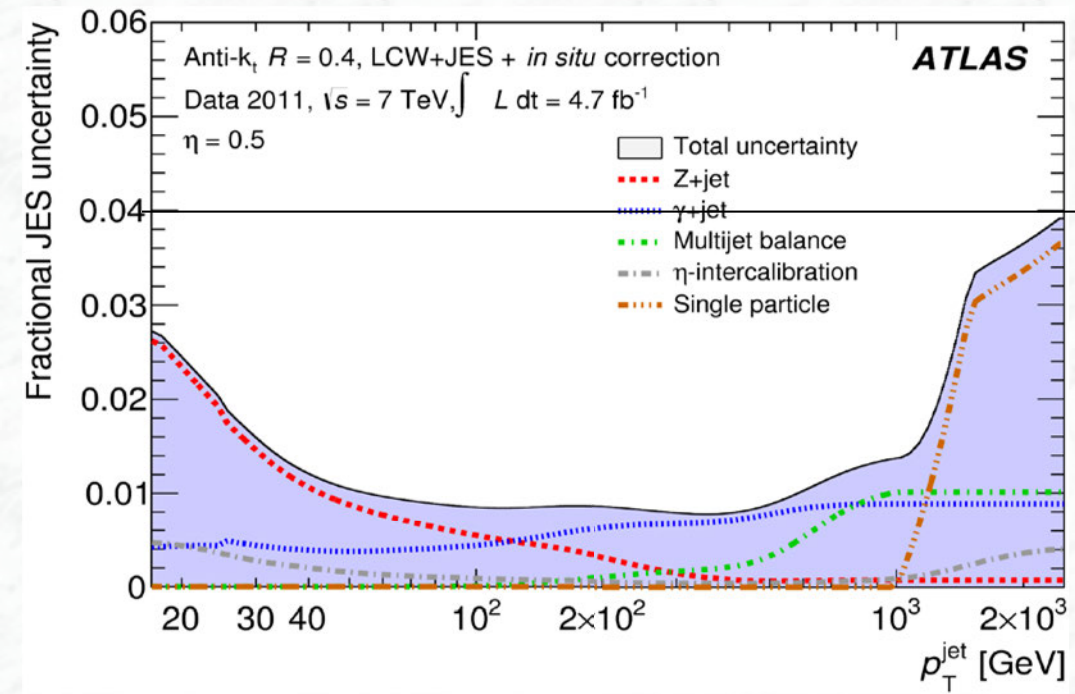
Electron ID efficiency in ATLAS



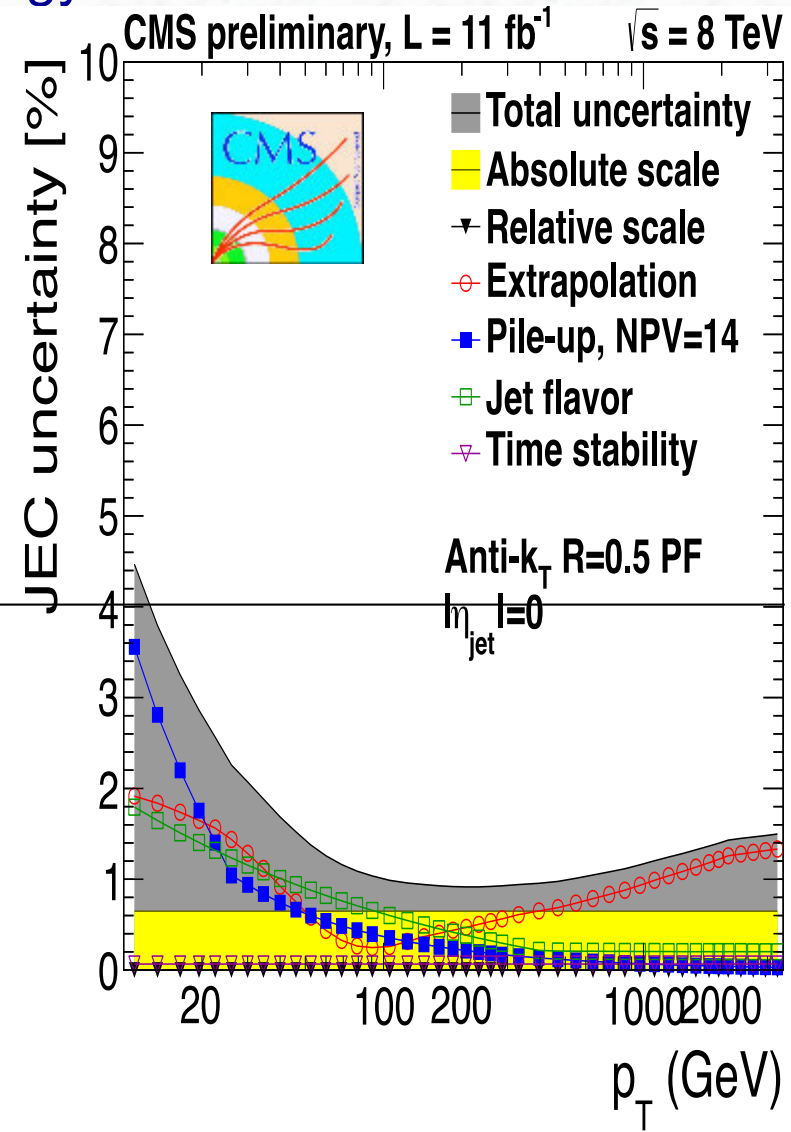
An example of a two-jet event reconstructed in ATLAS



(iv) Some performance figures on jet-energy scale from 2011 data:

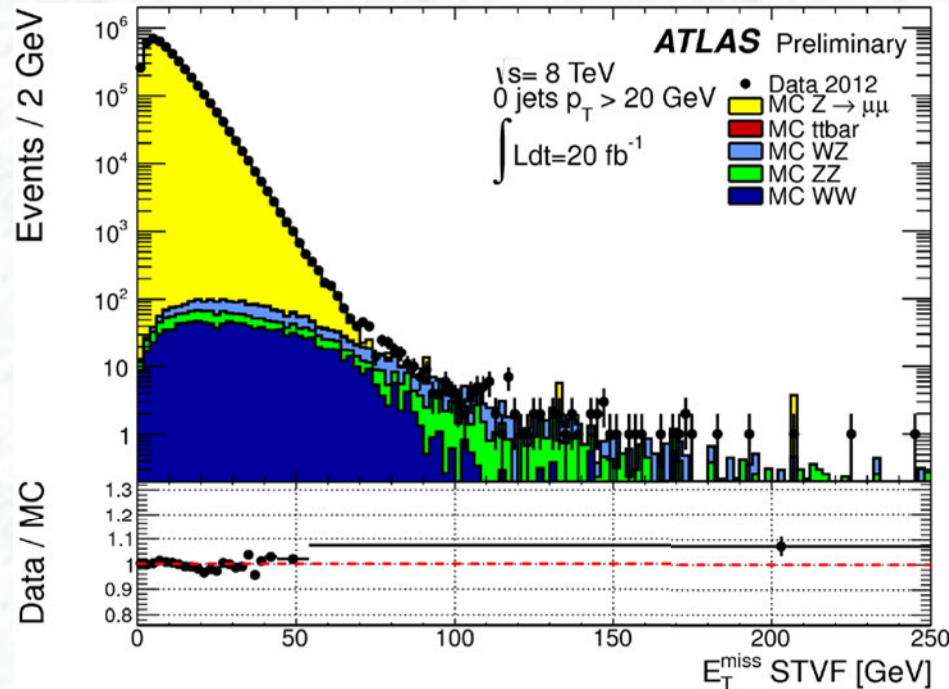


Jet energy scale (calorimetric) in ATLAS

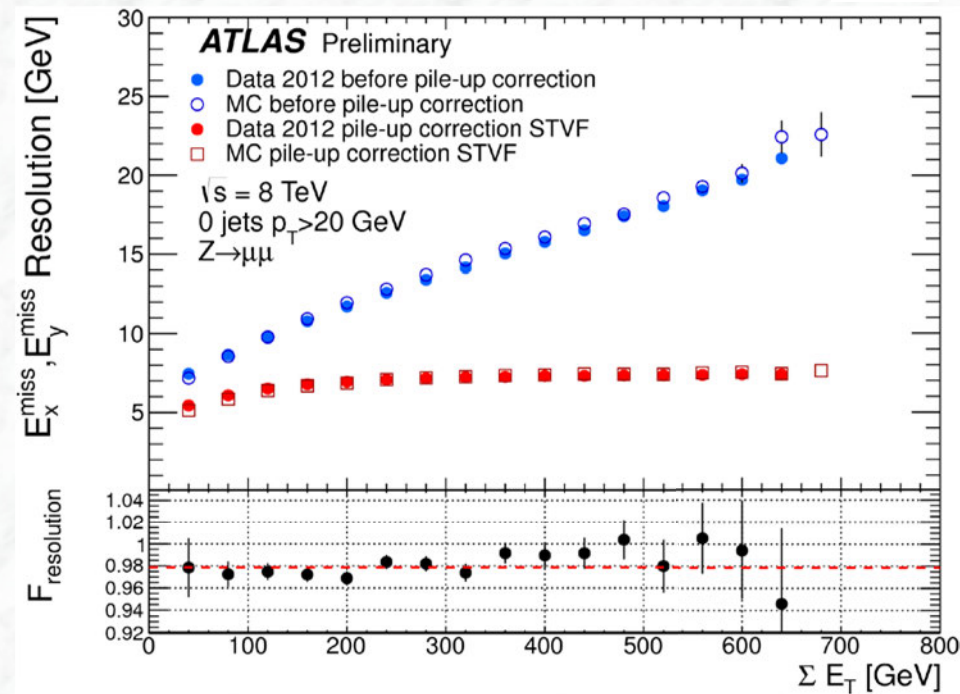


Jet energy scale,
particle-flow in CMS

(v) How well can the missing transverse energy be measured ?



Distribution of E_T^{miss} as measured in a data sample of $Z \rightarrow \mu\mu$ events. The expectation from Monte Carlo simulation is superimposed (histogram) and normalized to data, after each Monte Carlo sample is weighted with its corresponding cross-section. The ratio of the data distribution and the Monte Carlo distribution is shown below the plot.



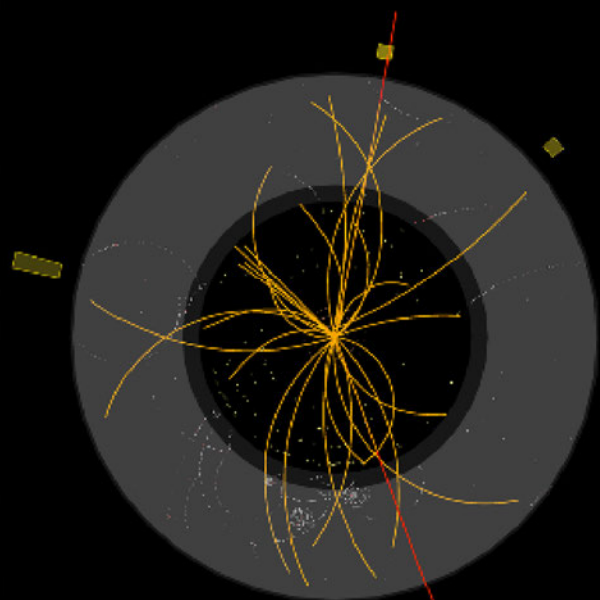
Resolution of E_x^{miss} and E_y^{miss} as a function of the total transverse energy in the event calculated by summing the p_T of muons and the total calorimeter energy. The resolution in $Z \rightarrow \mu\mu$ events is compared between data taken at $\sqrt{s} = 7 \text{ TeV}$ and the corresponding Monte Carlo.

$$\sigma(E_{x,y}^{\text{miss}}) = a \oplus b \sqrt{\sum E_T}$$

(vi) Muons

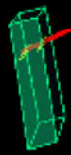


Run: 154822, Event: 14321500
Date: 2010-05-10 02:07:22 CEST

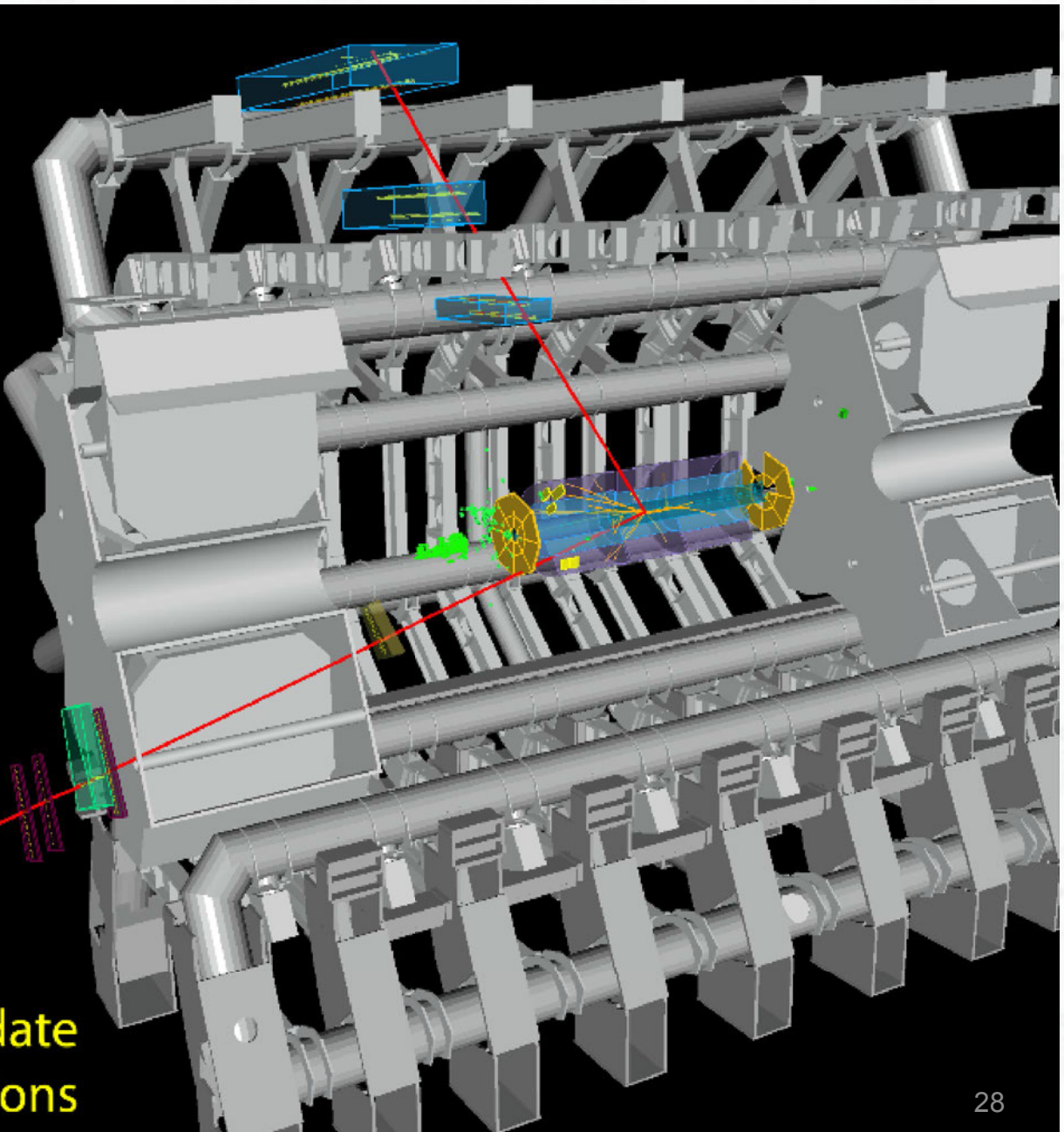


$$p_T(\mu^-) = 27 \text{ GeV} \quad \eta(\mu^-) = 0.7 \\ p_T(\mu^+) = 45 \text{ GeV} \quad \eta(\mu^+) = 2.2$$

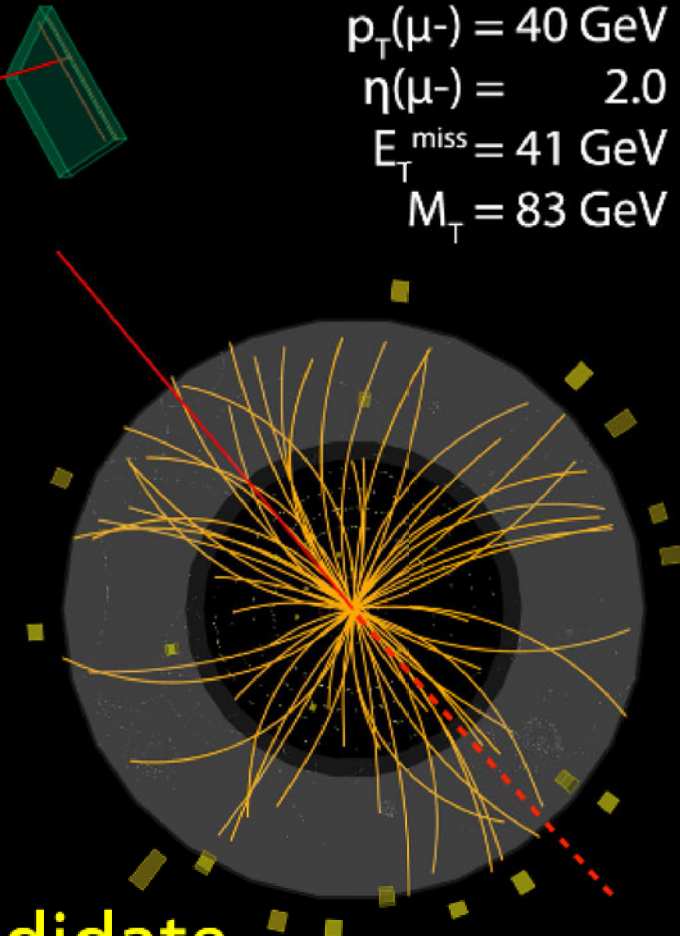
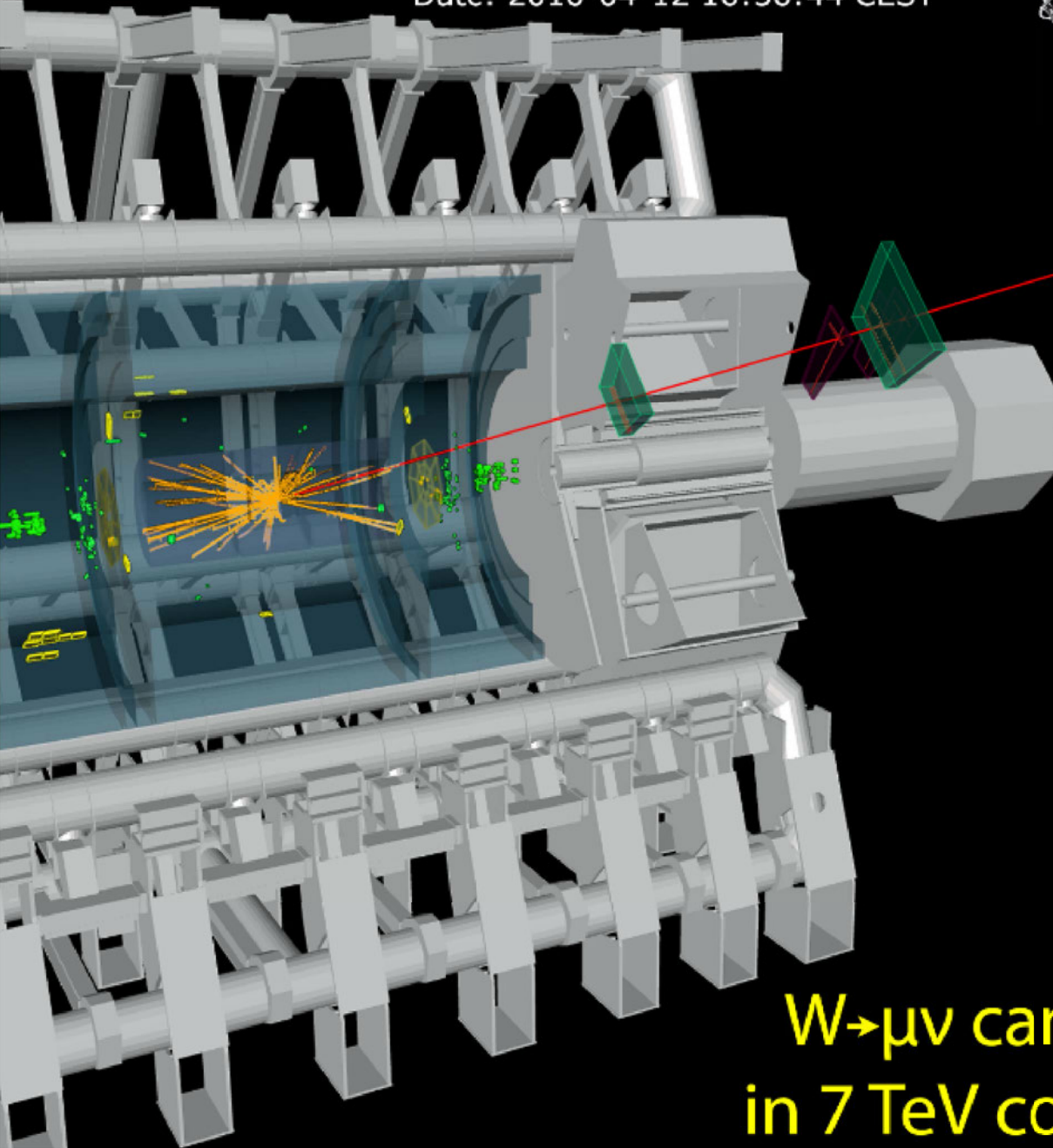
$$M_{\mu\mu} = 87 \text{ GeV}$$



Z \rightarrow $\mu\mu$ candidate
in 7 TeV collisions



Run: 152845, Event: 3338173
Date: 2010-04-12 16:56:44 CEST

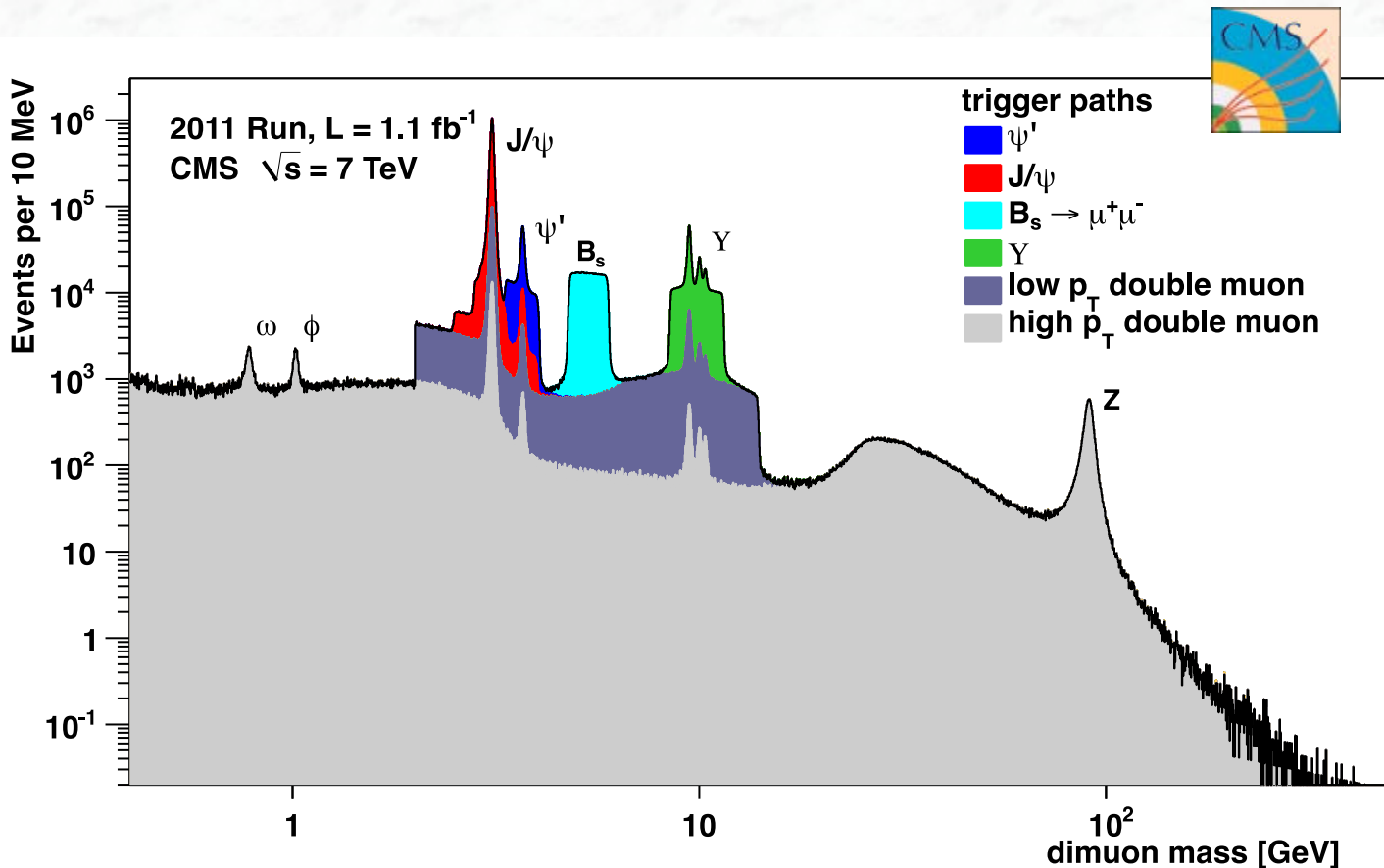


$W \rightarrow \mu\nu$ candidate
in 7 TeV collisions

$\mu^+\mu^-$ mass spectrum

Well known resonances. Observed widths depend on p_T resolution.

Again, check for biases in mass value as a function of η , ϕ , p_T ...



Observe influence of dedicated trigger paths

3.3 Relativistic Kinematics

Throughout this section, natural units are used, i.e. $\hbar = c = 1$.

The following conversions are useful:

$$\begin{aligned}\hbar c &= 197.3 \text{ MeV fm} \\ (\hbar c)^2 &= 0.3894 (\text{GeV})^2\end{aligned}$$

Lorentz Transformations

$$4\text{-vector } p = (E, \vec{p}) \quad p^2 \equiv E^2 - |\vec{p}|^2 = m^2$$

$$\text{velocity of the particle} \quad \beta = |\vec{p}| / E$$

(E^*, \vec{p}^*) viewed from a frame moving with velocity β

$$\begin{pmatrix} E^* \\ p_{\parallel}^* \end{pmatrix} = \begin{pmatrix} \gamma & -\gamma\beta \\ -\gamma\beta & \gamma \end{pmatrix} \begin{pmatrix} E \\ p_{\parallel} \end{pmatrix}, \quad p_T^* = p_T \quad \gamma = \frac{1}{\sqrt{1-\beta^2}}$$

where $p_T (p_{\parallel})$ are the components of \vec{p} perpendicular (parallel) to β

Lorentz Transformations (cont.)

Other 4-vectors transform in the same way:

e.g. space-time vectors $x = (t, \mathbf{x})$

Scalar products of four-vectors are Lorentz invariant,
independent of the reference frame:

$$p_1 \cdot p_2 = E_1 E_2 - \vec{p}_1 \cdot \vec{p}_2$$

Therefore quantities like cross sections are expressed in terms of scalar
products of four-vectors.

Centre-of-mass energy

- In the collision of two particles with masses m_1 and m_2 the total centre-of-mass energy can be expressed in the Lorentz-invariant form:

$$\begin{aligned} E_{cm} &= \left[(E_1 + E_2)^2 - (\mathbf{p}_1 + \mathbf{p}_2)^2 \right]^{1/2}, \\ &= \left[m_1^2 + m_2^2 + 2E_1 E_2 (1 - \beta_1 \beta_2 \cos \theta) \right]^{1/2} \end{aligned}$$

where θ is the angle between the particles.

Laboratory Frame

In the laboratory frame, one of the particles, e.g. particle 2, is at rest. The centre-of-mass energy is then given by:

$$E_{cm} = (m_1^2 + m_2^2 + 2E_{1lab}m_2)^{1/2}$$

The velocity of the centre-of-mass system in the lab frame is:

$$\beta_{cm} = \mathbf{p}_{lab} / (E_{1lab} + m_2),$$

where $\mathbf{p}_{lab} \equiv \mathbf{p}_{1lab}$ and $\gamma_{cm} = (E_{1lab} + m_2) / E_{cm}$

The centre-of-mass momenta of particles 1 and 2 are of magnitude

$$p_{cm} = p_{lab} \frac{m_2}{E_{cm}}.$$

Examples

- A beam of K^+ mesons with a momentum of 800 MeV hits a proton target at rest.

$$m_K = 493.7 \text{ MeV}, m_p = 938 \text{ MeV}, p_K = 0.80 \text{ GeV}$$

Then the centre-of-mass energy is calculated to be: $E_{cm} = 1.699 \text{ GeV}$
 $p_{cm} = 0.442 \text{ GeV}$

- At the LHC protons collide in their centre-of-mass system with a centre-of-mass energy of 14 TeV.

This corresponds to an energy of an incoming proton in a fixed target experiment (protons on protons) of $\sim 10^{17} \text{ GeV}$

(such energies can only be reached in cosmic rays!
but flux is not high enough to produce large numbers of interesting particles)

Comparison with cosmic rays

Primary cosmic ray spectrum

E spectrum falls as $E^{-2.7}$
to knee at $E \approx 5 \times 10^{15}$ eV
 $= 5 \times 10^6$ GeV
 ~ 1 particle/m² and year
origin galactic

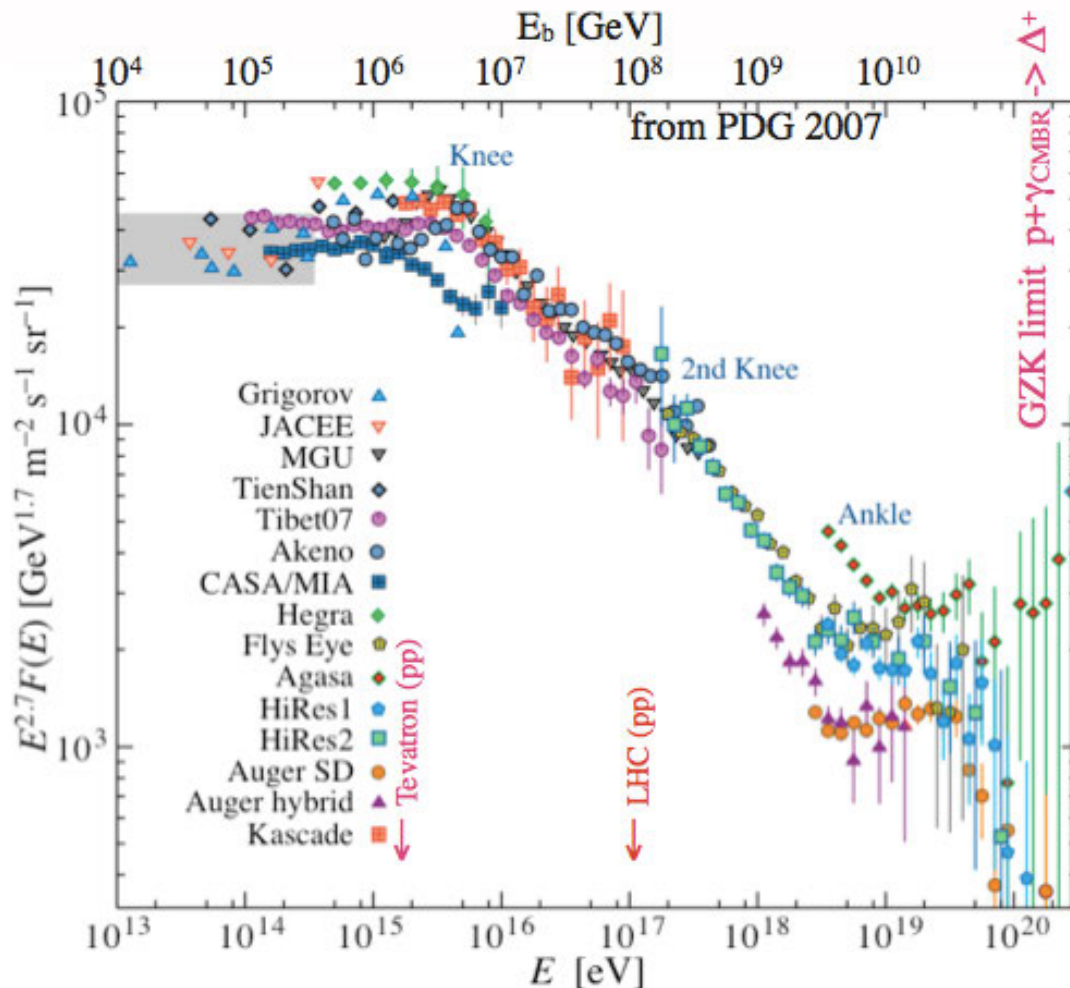
above $\sim E^{-3}$

back to $E^{-2.7}$ at very highest energies

conversion to E_{cm}

| E_b [eV] | E_{cm} [TeV] |
|------------|-----------------|
| 10^{13} | 0.137 |
| 10^{15} | 1.370 |
| 10^{17} | 13.70 \approx |
| 10^{19} | 137.0 |
| 10^{21} | 1370. |

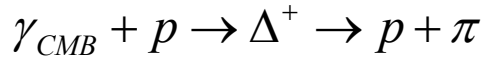
LHC



⇒ existance of **very powerful cosmic accelerators**. How do they work ?

GZK (Greisen-Zatsepin-Kuzmin) Limit

The sharp drop in the cosmic ray spectrum at 10^{20} eV is explained by interactions of protons with photons from cosmic background radiation



$$E_\gamma = kT = 2.6 \cdot 10^{-4} \text{ eV} (T = 3 \text{ K})$$

$$E_p = 1 \cdot 10^{20} \text{ eV}$$

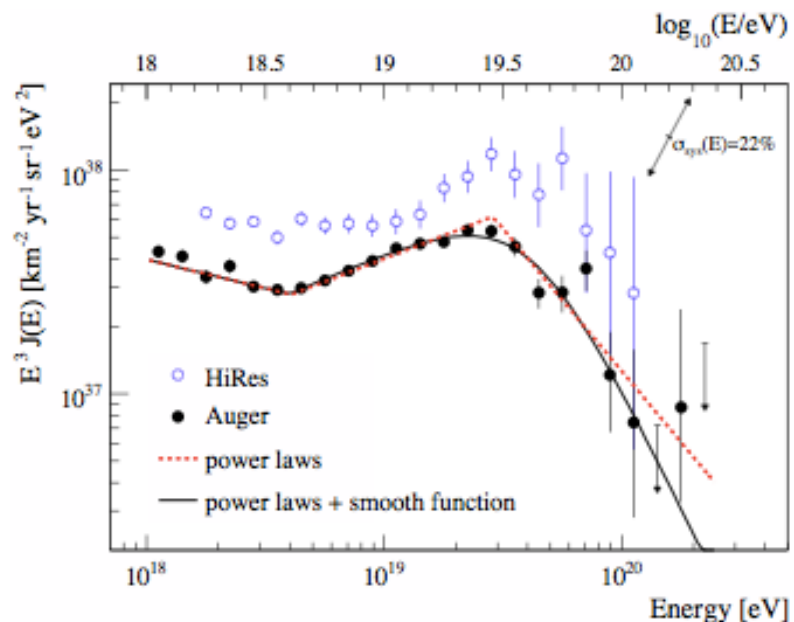
$$E_{cms} \approx 1 \text{ GeV}$$

At CMS energies around 1 GeV the cross sections for π -production through the Δ -resonance becomes large. Thus protons loose energy.

Cosmic protons at this energy have a mean free path of **160 MLy** (GZK horizon). Thus extragalactic protons with energies larger than 10^{20} eV should not reach the earth. Recent measurements of the Auger experiment confirm this cut-off.

Auger Experiment

<http://arxiv.org/abs/1002.1975v1>



The combined energy spectrum is dotted with two functions and compared to data from the HiRes instrument. The systematic uncertainty of the flux scaled by E^3 due to the uncertainty of the energy scale of 22% is indicated by arrows.

Lorentz invariant amplitudes

The matrix elements for the scattering or decay process are written in terms of an invariant amplitude $-i M$. As an example, the S-matrix for $2 \rightarrow 2$ scattering is related to M by

$$\begin{aligned} \langle p_1' p_2' | S | p_1 p_2 \rangle &= I - i(2\pi)^4 \delta^4(p_1 + p_2 - p_1' - p_2') \\ &\times \frac{M(p_1, p_2; p_1', p_2')}{(2E_1)^{1/2} (2E_2)^{1/2} (2E_1')^{1/2} (2E_2')^{1/2}} \end{aligned}$$

The normalization is such that $\langle p' | p \rangle = (2\pi)^3 \delta^3(\mathbf{p} - \mathbf{p}')$

The task is to calculate the invariant amplitude M for a given physics process. In particle physics this is achieved using the Feynman calculus (see lecture on Particle Physics II)

Particle Decays

The **partial decay rate** of a particle of mass m into n bodies in its rest frame is given in terms of the Lorentz-invariant matrix element M by

$$d\Gamma = \frac{(2\pi)^4}{2m} |M|^2 d\Phi_n(P; p_1, \vec{p}_2, \dots, \vec{p}_n)$$

where $d\Phi_n$ is an element of **n-body phase space** given by:

$$d\Phi_n(P; p_1, \vec{p}_2, \dots, \vec{p}_n) = \delta^4(P - \sum_{i=1}^n p_i) \prod_{i=1}^n \frac{d^3 p_i}{(2\pi)^3 2E_i}$$

Survival probability of Decay

If a particle of mass m has a mean proper lifetime of τ ($=1/\Gamma$) and an energy-momentum 4-vector of (E, \mathbf{p}) , then the probability that it lives for a time t or greater before decaying is given by

$$P(t) = e^{-t/\tau} = e^{-mt\Gamma/E}$$

and the probability that it travels a distance x or greater is

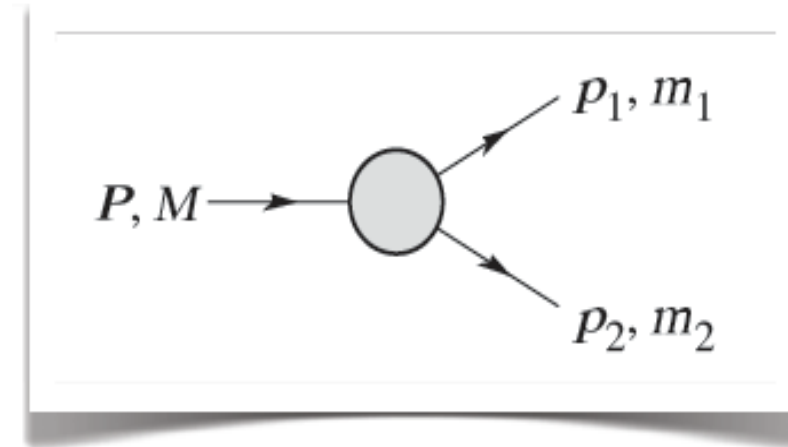
$$P(x) = e^{-mx\Gamma/|p|}$$

Example (i): Two-Body Decay

In the rest frame of a particle of mass m , decaying into two particles labelled 1 and 2

$$E_1 = \frac{m^2 - m_2^2 + m_1^2}{2m},$$
$$|p_1| \neq |p_2|$$
$$= \frac{\left[(m^2 - (m_1 + m_2)^2)(m^2 - (m_1 - m_2)^2) \right]^{1/2}}{2m},$$

$$d\Gamma = \frac{1}{32\pi^2} |M|^2 \frac{|p_1|}{m^2} d\Omega,$$



where $d\Omega = d\phi_1 d(\cos\theta_1)$ is the solid angle of particle 1

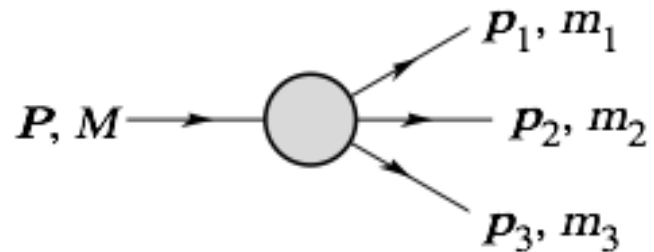
The invariant mass m of the mother particle in a two-body decay is given by $m = E_{cm}$ using the previous formula:

$$\begin{aligned}E_{cm} &= \left[(E_1 + E_2)^2 - (p_1 + p_2)^2 \right]^{1/2} \\&= \left[m_1^2 + m_2^2 + 2E_1 E_2 (1 - \beta_1 \beta_2 \cos \theta) \right]^{1/2}\end{aligned}$$

Generalisation: the invariant mass of n particles is given by:

$$m = (p_1 + p_2 + p_3 + \dots + p_n)^2$$

Example (ii): Three-Body Decay



Defining $p_{ij} = p_i + p_j$ and $m^2_{ij} = p_{ij}^2$

$$\text{then } m^2_{12} + m^2_{23} + m^2_{13} = m^2 + m^2_1 + m^2_2 + m^2_3$$

$$\text{and } m^2_{12} = (\mathbf{P} - \mathbf{p}_3)^2 = m^2 + m^2_3 - 2 m E_3$$

E_3 is the energy of particle 3 in the rest frame of m .

In that frame, the momenta of the three decay particles lie in a plane.

The relative orientation of these three momenta is fixed if their energies are known. The momenta can therefore be specified in space by giving three Euler angles (α, β, γ) that specify the orientation of the final system relative to the initial particle

$$d\Gamma = \frac{1}{(2\pi)^5} \frac{1}{16M} |M|^2 dE_1 dE_2 d\alpha d(\cos \beta) d\gamma$$

Alternatively

$$d\Gamma = \frac{1}{(2\pi)^5} \frac{1}{16M^2} |M|^2 |\mathbf{p}_1^*| |\mathbf{p}_3| dm_{12} d\Omega_1^* d\Omega_3$$

where $(|\mathbf{p}_1^*|, \Omega_1^*)$ is the momentum of particle 1 in the rest frame of 1 and 2, and Ω_3 is the angle of particle 3 in the rest frame of the decaying particle.

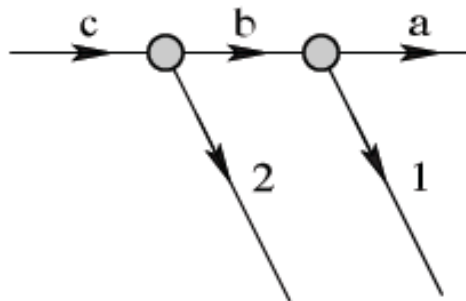
Three-Body Decay (cont.)

$| p_1^* |$ and $| p_3 |$ are given by

$$| p_1^* | = \frac{[(m_{12}^2 - (m_1 + m_2)^2)(m_{12}^2 - (m_1 - m_2)^2)]^{1/2}}{2m_{12}}$$

$$| p_3 | = \frac{[(m^2 - (m_{12} + m_3)^2)(m^2 - (m_{12} - m_3)^2)]^{1/2}}{2m}$$

Sequential 2-Body Decays



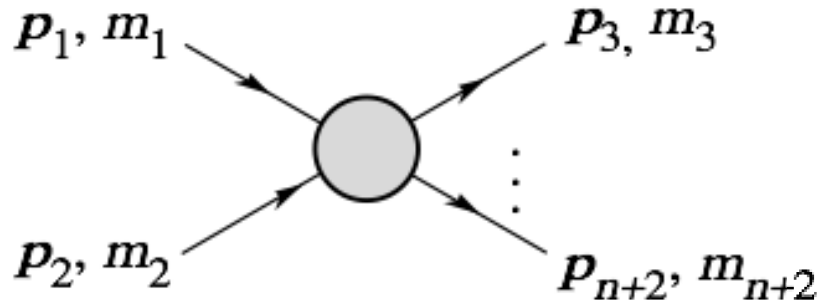
Particles participating in sequential two-body decay chain. Particles labeled 1 and 2 are visible while the particle terminating the chain (a) is invisible.

$$(m_{12}^{\max})^2 = \frac{(m_c^2 - m_b^2)(m_b^2 - m_a^2)}{m_b^2}, \text{ provided particles 1 and 2 are massless.}$$

$$(m_{12}^{\max})^2 = m_1^2 + \frac{(m_c^2 - m_b^2)}{2m_b^2} \times \\ \left(m_1^2 + m_b^2 - m_a^2 + \sqrt{(-m_1^2 + m_b^2 - m_a^2)^2 - 4m_1^2 m_a^2} \right).$$

If visible particle 1
has non-zero mass m_1

Differential Cross Section



$$d\sigma = \frac{(2\pi)^4 |\mathcal{M}|^2}{4\sqrt{(p_1 \cdot p_2)^2 - m_1^2 m_2^2}} \times d\Phi_n(p_1 + p_2; p_3, \dots, p_{n+2}) .$$

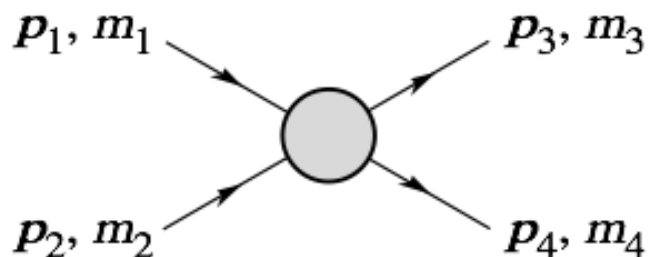
In the rest frame of m_2 (lab)

$$\sqrt{(p_1 \cdot p_2)^2 - m_1^2 m_2^2} = m_2 p_{1\text{ lab}}$$

In the centre-of-mass frame

$$\sqrt{(p_1 \cdot p_2)^2 - m_1^2 m_2^2} = p_{1\text{cm}} \sqrt{s}$$

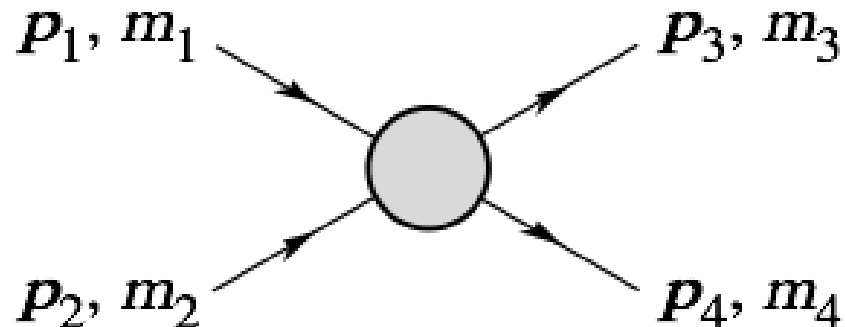
Mandelstam Variables (two-to-two process)



$$\begin{aligned}s &= (p_1 + p_2)^2 = (p_3 + p_4)^2 \\&= m_1^2 + 2E_1 E_2 - 2\mathbf{p}_1 \cdot \mathbf{p}_2 + m_2^2 , \\t &= (p_1 - p_3)^2 = (p_2 - p_4)^2 \\&= m_1^2 - 2E_1 E_3 + 2\mathbf{p}_1 \cdot \mathbf{p}_3 + m_3^2 , \\u &= (p_1 - p_4)^2 = (p_2 - p_3)^2 \\&= m_1^2 - 2E_1 E_4 + 2\mathbf{p}_1 \cdot \mathbf{p}_4 + m_4^2 ,\end{aligned}$$

$$s + t + u = m_1^2 + m_2^2 + m_3^2 + m_4^2 .$$

Cross section



Using the relations given above, the two-body cross section can be written as:

$$\frac{d\sigma}{dt} = \frac{1}{64\pi s} \frac{1}{|\mathbf{p}_{1\text{cm}}|^2} |\mathcal{M}|^2$$

Advantage to use Lorentz invariant quantities, like t .

The variable t is given by:

$$\begin{aligned} t &= (E_{1\text{cm}} - E_{3\text{cm}})^2 - (p_{1\text{cm}} - p_{3\text{cm}})^2 - 4p_{1\text{cm}} p_{3\text{cm}} \sin^2(\theta_{\text{cm}}/2) \\ &= t_0 - 4p_{1\text{cm}} p_{3\text{cm}} \sin^2(\theta_{\text{cm}}/2) \end{aligned}$$

where θ_{cm} is the angle between particle 1 and 3.

The limiting values t_0 ($\theta_{\text{cm}} = 0$) and t_1 ($\theta_{\text{cm}} = \pi$) for 2→2 scattering are

$$t_0(t_1) = \left[\frac{m_1^2 - m_3^2 - m_2^2 + m_4^2}{2\sqrt{s}} \right]^2 - (p_{1\text{cm}} \mp p_{3\text{cm}})^2$$

The centre-of-mass energies and momenta of the incoming particles are

$$E_{1\text{cm}} = \frac{s + m_1^2 - m_2^2}{2\sqrt{s}}, \quad E_{2\text{cm}} = \frac{s + m_2^2 - m_1^2}{2\sqrt{s}}$$

For $E_{3\text{cm}}$ and $E_{4\text{cm}}$, change m_1 to m_3 and m_2 to m_4 (same particles).

$$p_{i\text{cm}} = \sqrt{E_{i\text{cm}}^2 - m_i^2} \text{ and } p_{1\text{cm}} = \frac{p_{1\text{lab}} m_2}{\sqrt{s}}$$

Here the subscript lab refers to the frame where particle 2 is at rest.

3.4 Important kinematic Variables in pp collisions

(i) Rapidity y

Usually the beam direction is defined as the z axis (Transverse plane: x - y plane).

The rapidity y is defined as:

$$y = \frac{1}{2} \ln \left(\frac{E + p_z}{E - p_z} \right) = \tanh^{-1} \left(\frac{p_z}{E} \right)$$

Under a **Lorentz boost** in the z -direction to a frame with velocity β

the rapidity y transforms as: $y \rightarrow y - \tanh^{-1} \beta$

Hence the shape of the rapidity distribution dN/dy is invariant, as are differences in rapidity.

(ii) Pseudorapidity η

Rapidity: $y = \frac{1}{2} \ln \left(\frac{E + p_z}{E - p_z} \right) = \tanh^{-1} \left(\frac{p_z}{E} \right)$

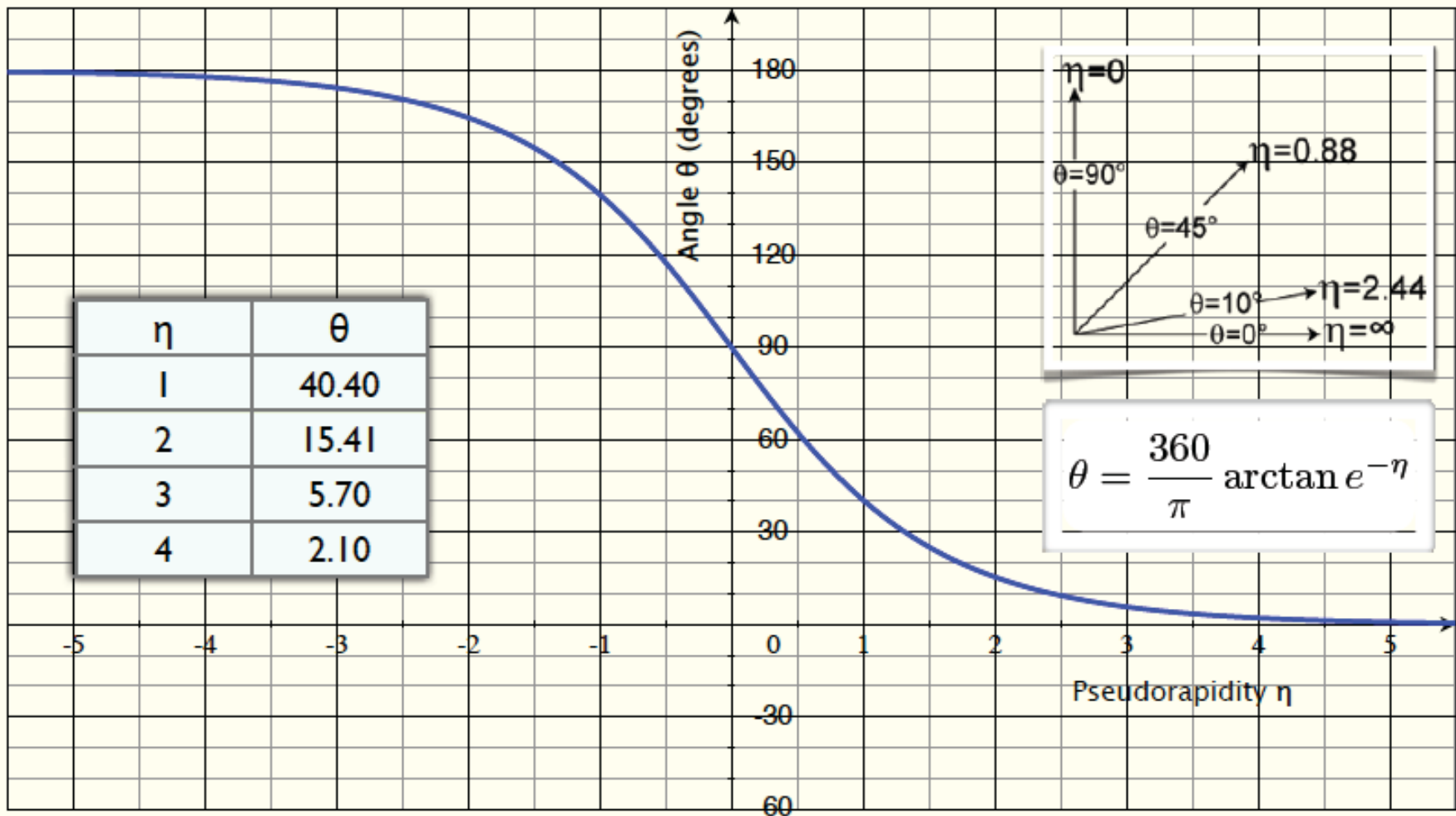
For $p \gg m$, the rapidity may be expanded to obtain

$$y = \frac{1}{2} \ln \frac{\cos^2(\theta/2) + m^2/4p^2 + \dots}{\sin^2(\theta/2) + m^2/4p^2 + \dots}$$
$$\approx -\ln \tan(\theta/2) \equiv \eta$$

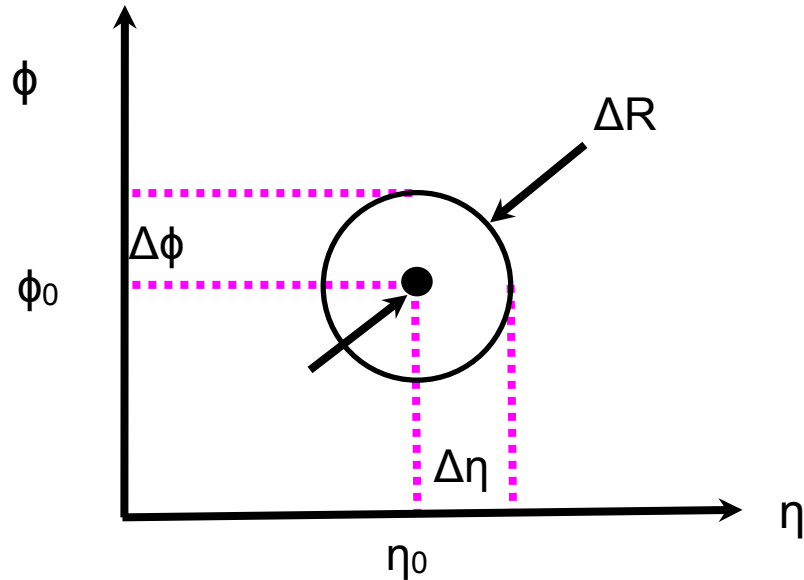
where $\cos \theta = p_z/p$.

Identities: $\sinh \eta = \cot \theta$, $\cosh \eta = 1/\sin \theta$, $\tanh \eta = \cos \theta$

Relation between pseudorapidity η and polar angle θ



(iii) Distance in $\eta \square \phi$ space:



Rapidity y : $y = 1/2 \ln[(E + p_z)/(E - p_z)]$

Pseudorapidity η : $\eta = -\ln \tan(\theta/2)$

Distance in η - ϕ : $\Delta R = \sqrt{\Delta\eta^2 + \Delta\phi^2}$

(iv) Invariant cross section

The invariant cross section may also be rewritten

$$E \frac{d^3\sigma}{d^3p} = \frac{d^3\sigma}{d\phi dy p_T dp_T} \implies \frac{d^2\sigma}{\pi dy d(p_T^2)}$$

The second form is obtained using the identity $dy/dp_z = 1/E$.

The third form represents the average over ϕ .

(v) Transverse Energy

At hadron colliders, a significant and unknown proportion of the energy of the incoming hadrons in each event escapes down the beam-pipe. Consequently if invisible particles are created in the final state, their net momentum can only be constrained in the plane transverse to the beam direction. Defining the z-axis as the beam direction, this net momentum is equal to the missing transverse energy vector

missing transverse energy

$$\vec{E}_T^{\text{miss}} = - \sum_i \vec{p}_T(i)$$

where the sum runs over the transverse momenta of all visible final state particles.

(vi) Momenta of invisible particles

Consider a single heavy particle of mass M produced in association with visible particles which decays to two particles, of which one (labelled particle 1) is invisible. The mass of the parent particle can be constrained with the quantity M_T defined by

Transverse mass

$$\begin{aligned} M_T^2 &\equiv [E_T(1) + E_T(2)]^2 - [\vec{p}_T(1) + \vec{p}_T(2)]^2 \\ &= m_1^2 + m_2^2 + 2[E_T(1)E_T(2) - \vec{p}_T(1) \cdot \vec{p}_T(2)] \end{aligned}$$

where

$$\vec{p}_T(1) = \vec{E}_T^{\text{miss}}$$

This quantity is called the **transverse mass**.

Transverse mass

$$\begin{aligned} M_T^2 &\equiv [E_T(1) + E_T(2)]^2 - [\vec{p}_T(1) + \vec{p}_T(2)]^2 \\ &= m_1^2 + m_2^2 + 2[E_T(1)E_T(2) - \vec{p}_T(1) \cdot \vec{p}_T(2)] \end{aligned}$$

where $\vec{p}_T(1) = \vec{E}_T^{\text{miss}}$

The distribution of event M_T values possesses an end-point at

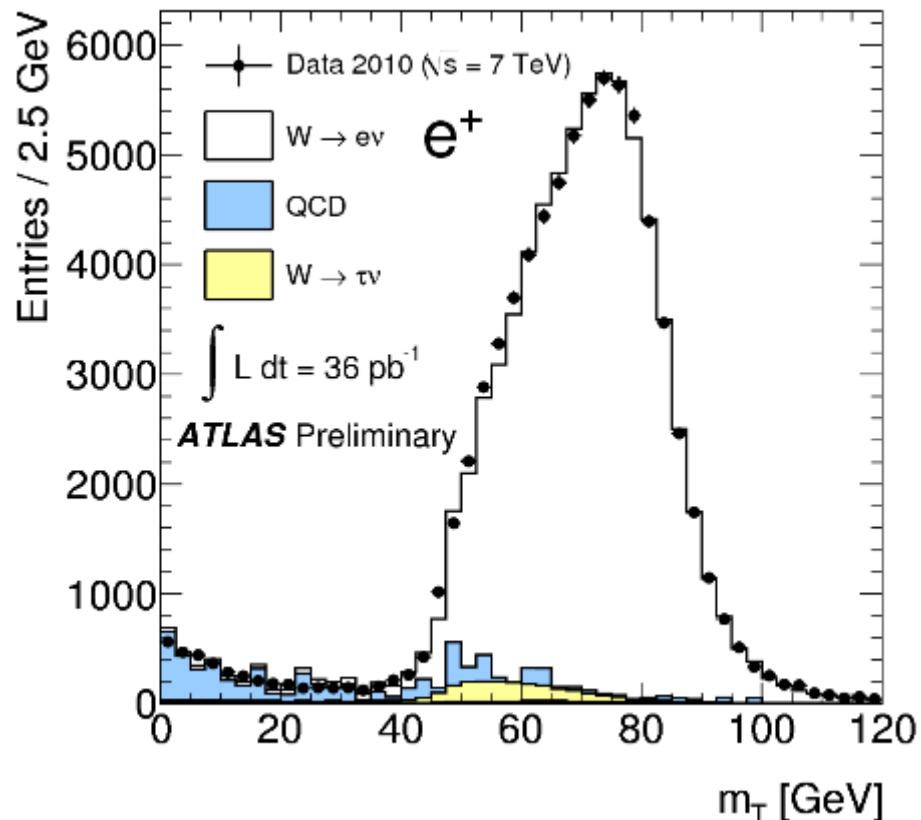
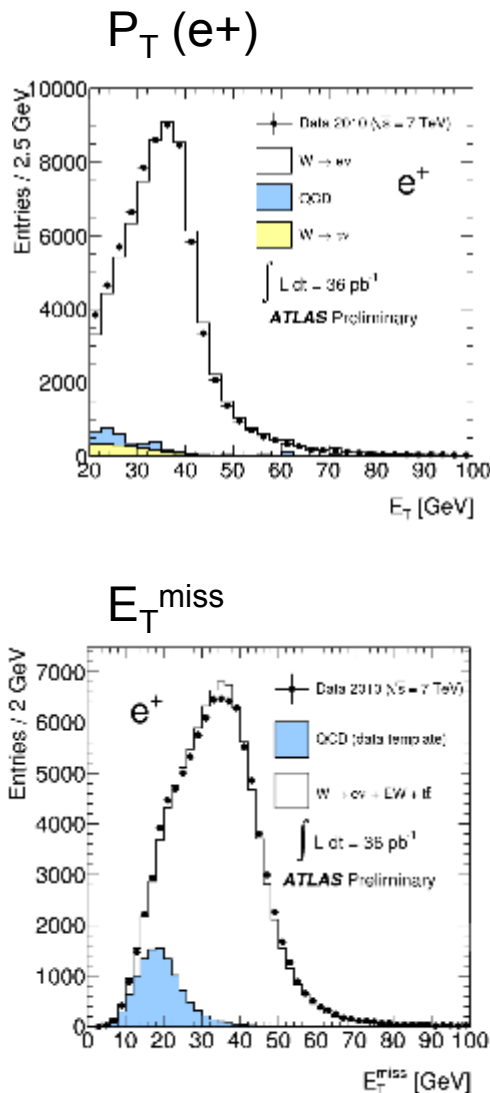
$$M_T^{\max} = \bar{M}.$$

If $m_1 = m_2 = 0$

$$M_T^2 = 2|\vec{p}_T(1)||\vec{p}_T(2)|(1 - \cos \phi_{12})$$

where ϕ_{ij} is defined as the angle between particles i and j in the transverse plane.

Example: Transverse mass of the W boson



$$m_T = \sqrt{2 P_T(e) E_T^{\text{miss}} (1 - \cos \Delta\phi)}$$

(see previous slide)